THE GENOMIC ARCHITECTURE OF A RAPID ISLAND RADIATION: RECOMBINATION RATE VARIATION, CHROMOSOME STRUCTURE, AND GENOME ASSEMBLY OF THE HAWAIIAN CRICKET *LAUPALA*

Thomas Blankers[1], Kevin P. Oh[1], Aureliano Bombarely[2], Kerry L. Shaw[1]

[1] *Department of Neurobiology and Behavior, Cornell University, Ithaca, NY, USA*

[2] *Department of Horticulture, Virginia Tech, Blacksburg, VA, USA*

12

13 **Running Title:** *Laupala* Genomic Architecture

14

15 **Key words:** speciation, sexual selection, recombination, chromosomal rearrangements, genome,

16 crickets

17

18

19 **Corresponding author:**

20 Thomas Blankers, Department of Neurobiology and Behavior, Cornell University, W319 215

21 Tower rd, 14850, Ithaca, NY, USA. thomasblankers@gmail.com. 1- (607) 254 4326

22

23

ABSTRACT

Phenotypic evolution and speciation depend on recombination in many ways. Within populations, recombination can promote adaptation by bringing together favorable mutations and decoupling beneficial and deleterious alleles. As populations diverge, cross-over can give rise to maladapted recombinants and impede or reverse diversification. Suppressed recombination due to genomic rearrangements, modifier alleles, and intrinsic chromosomal properties may offer a shield against maladaptive gene flow eroding co-adapted gene complexes. Both theoretical and empirical results support this relationship. However, little is known about this relationship in the context of behavioral isolation, where co-evolving signals and preferences are the major hybridization barrier. Here we examine the genomic architecture of recently diverged, sexually isolated Hawaiian swordtail crickets (*Laupala*). We assemble a *de novo* genome and generate three dense linkage maps from interspecies crosses. In line with expectations based on the species' recent divergence and successful interbreeding in the lab, the linkage maps are highly collinear and show no evidence for large-scale chromosomal rearrangements. The maps were then used to anchor the assembly to pseudomolecules and estimate recombination rates across the genome. We tested the hypothesis that loci involved in behavioral isolation (song and preference divergence) are in regions of low interspecific recombination. Contrary to our expectations, a genomic region where a male song QTL co-localizes with a female preference QTL was not associated with particularly low recombination rates. This study provides important novel genomic resources for an emerging evolutionary genetics model system and suggests that trait-preference co-evolution is not necessarily facilitated by locally suppressed recombination.

INTRODUCTION

Speciation is contingent on the accumulation of genomic variation and the formation of barriers that prevent gene flow between populations. Genomes diverge under the influence of selection and drift, while gene flow counteracts this divergence by homogenizing the genome (Felsenstein 1981; Kirkpatrick and Ravigne 2002; Gavrilets 2003). To appreciate the speciation process and the origin of the fascinating diversity of life on earth, we need to understand the interaction between the mechanisms that change allele frequencies and the mechanisms that govern the association of beneficial and deleterious alleles with other alleles. A key process in this interaction is recombination, which creates new allelic combinations during meiosis in sexually reproducing organisms.

Any association between loci that underlie environmental adaptation or between loci underlying co-evolving (sexual) signals and signal responses (i.e. co-adapted gene complexes) will be affected by recombination (Felsenstein 1981). Within populations, recombination can mitigate Hill-Robertson interference by combining locally adaptive alleles from different genomic backgrounds and by decoupling beneficial and deleterious alleles (Hill and Robertson 1966); recombination can also influence the covariance between sexual traits and preference across sexes (Smith and Haigh 1974; Smith 1978; Gillespie 2000; Otto 2009). As such, recombination might increase the efficiency of background selection (purging deleterious alleles), sexual selection (through signal-preference co-evolution), and local adaptation in the earliest stages of speciation (by linking locally adapted alleles; Noor *et al.* 2001; Rieseberg 2001; Kirkpatrick and Ravigne 2002; Yeaman and Whitlock 2011).

Between divergent populations with some (but incomplete) reproductive isolation, recombination can also counteract population divergence and prevent the closure of a reproductive boundary by

creating combinations of alleles that are favorable in different contexts (Noor *et al.* 2001; Rieseberg 2001; Coyne and Orr 2004; Ortiz-Barrientos *et al.* 2016). It is important to realize that interspecific recombination is constrained both by intrinsic properties of the species' genomes that also constrain intraspecific recombination, as well as by the effects from (divergent) selection and alternatively fixed chromosomal rearrangements (Yeaman and Whitlock 2011; Feder *et al.* 2012). The most intensely studied chromosomal rearrangements suppressing recombination between divergent populations are inversions. Inversions can suppress recombination locally in the genome and, thus, promote reproductive isolation, by trapping genetic incompatibilities in linkage blocks (Noor *et al.* 2001), acting synergistically with other genes causing isolation (Rieseberg 2001), or by linking locally adaptive alleles (Kirkpatrick and Barton 2006). Other chromosomal rearrangements, such as translocations and transposable elements, can likewise contribute to 'chromosomal speciation' (Rieseberg 2001) as well as to preventing gene flow and furthering genetic divergence among heterospecifics.

Interestingly, there is ubiquitous among-species variation in recombination rates (Wilfert *et al.* 2007; Smukowski and Noor 2011). In insects, for example, rates vary from 16.1 cM/Mb (centi-Morgans per megabase) in *Apis melifera* to 0.1 cM/Mb in the mosquito *Armigeres subalbatus* (Wilfert *et al.* 2007). There is also variation across the genome within individuals. For example, 50-fold differences have been observed within single chromosomes of humans and birds (Myers *et al.* 2005; Singhal *et al.* 2015). These patterns of variation underline that the efficacy of selection acting within species may differ across taxa and across genomes of the same species.

A major prediction following from theoretical work is that favorable allele combinations that promote ecological adaptation are more likely to reside in regions of low recombination. Recombination frustrates natural selection by breaking up associations between segregating

93 alleles that are locally adaptive within the resident population and counteracts divergent selection
94 if there is gene flow between recently diverged populations (Bürger and Akerman 2011; Yeaman
95 and Whitlock 2011; Yeaman 2013). So far, empirical evidence for the prediction that locally
96 adaptive alleles reside in regions of low recombination is not conclusive (Roesti *et al.* 2013;
97 Burri *et al.* 2015; Marques *et al.* 2016). However, a recent study indicated that the interaction
98 between gene flow and divergent selection is a strong predictor for the association between
99 adaptive alleles and regions of low recombination in multiple species of stickleback fish (Samuk
100 *et al.* 2017).

101 However, it is unclear how these predictions apply to the evolution of behavioral isolation.
102 Theoretical models of speciation by sexual selection depend on linkage disequilibrium between
103 sexual signaling traits and corresponding preference genes (Fisher 1930; Lande 1981;
104 Kirkpatrick 1982). Linkage disequilibrium between trait and preference genes can come about by
105 assortative mating (Lande 1981; Andersson and Simmons 2006) or by physical linkage
106 (Kirkpatrick and Hall 2004), either through closely linked loci or through pleiotropy (a single
107 gene affecting both signal and preference phenotypes). Here, the role of recombination is more
108 complex: On the one hand, recombination can help consolidate loci brought together by
109 nonrandom mating and as such facilitate linkage disequilibrium between trait and preference
110 (Kirkpatrick and Ravigne 2002). On the other hand, recombination can also tear apart co-adapted
111 trait and preference alleles if genes are exchanged between populations that differ in mating
112 phenotypes. Therefore, recombination between sexually divergent populations in sympatry and
113 parapatry often compromises differentiation in mating phenotypes and hinders speciation
114 (Arnegard *et al.* 2004; Servedio 2009, 2015; Servedio and Burger 2014). However, there has

115 been limited empirical insight into the relationship between trait-preference co-evolution and
116 genome-wide variation in recombination rates (see Davey *et al.* 2017 for a recent exception).

117 Here, we examine the genomic architecture, specifically structural variation and heterogeneity in
118 interspecific recombination, of four closely related, sexually isolated species of Hawaiian
119 swordtail crickets from the genus *Laupala*. *Laupala* is one of the fastest speciating taxa known to
120 date (Mendelson and Shaw 2005). The 38 morphologically cryptic species, each endemic to a
121 single island of the Hawaiian archipelago (Otte 1994; Shaw 2000a) are the product of a recent
122 evolutionary radiation. Evidence suggests that speciation by sexual selection on the acoustic
123 communication system has driven this rapid diversification, as both male mating song and
124 female acoustic preferences have diverged extensively among *Laupala* species (Otte 1994; Shaw
125 2000b; Mendelson and Shaw 2002). Sexual trait evolution strongly contributes to the onset and
126 maintenance of reproductive isolation (Mendelson and Shaw 2002; Grace and Shaw 2011).
127 Quantitative variation in one key temporal property of male song (pulse rate) and corresponding
128 female preference strongly covaries across species and across populations within species (Shaw
129 2000b; Grace and Shaw 2011). Although the mechanisms of trait-preference co-evolution require
130 further study, there is evidence that both are associated with a polygenic basis and that genetic
131 loci controlling quantitative variation in traits and preferences are physically linked in the
132 genome (Shaw and Lesnick 2009; Wiley *et al.* 2012). Notably, one of the major song
133 quantitative trait loci (QTL; haploid effect size ~ 9%) co-localizes with the first mapped
134 preference QTL (haploid effect size ~ 14%). Directional effects of song QTL provide additional
135 evidence that (sexual) selection is driving divergence between species (Shaw *et al.* 2007).

136 The species pairs involved in this study, *L. kohalensis* and *L. pruna*, and *L. paranigra* and *L.*
137 *kona*, are endemic to the Big Island, the youngest island of the Hawaiian archipelago (Fig 1A,

B). Although these species pairs have apparently diverged in allopatry within the Big Island, past or future migration is likely, given their geographical proximity. Indeed, although allopatric and more closely related to *L. kohalensis*, *L. pruna* currently overlaps in distribution with *L. paranigra* (Fig 1B). The discordance between nuclear and mitochondrial phylogenies (Shaw 2002) and the limited degree of postzygotic isolation between some species pairs further emphasize the possibility of gene flow across natural populations. Together, the biogeography and the genetics of song and preference variation in this system provide a unique opportunity to explore the interaction between interspecific recombination rate variation, co-evolution of mating traits, and speciation.

We first assemble a *de novo L. kohalensis* draft genome and then obtain thousands of SNP markers for heterogeneously hybrid offspring from three laboratory-generated interspecific crosses. We then generate three dense linkage maps and compare these maps to test the hypothesis that the genomic architectures of young, sexually differentiated species are largely collinear (similar marker order) and have conserved interspecific recombination frequencies (similar marker distances). There is some variation in the level of overall differentiation in the species pairs studied here, but all lineages are young (approximately 0.5 million years or less, Fig 1). It is commonly expected that strong prezygotic isolation can evolve rapidly and largely in the absence of intrinsic postzygotic isolating mechanisms (Coyne and Orr 2004), but explicit comparisons of chromosomal architectures across behaviorally isolated species are rare. We compare the maps visually and use variation in maker order and length (measured in genetic distance, or centi-Morgans [cM]) as indicators of possible chromosomal rearrangements affecting the recombination rates differently in different crosses (Fig 1C). Then, from the large amount of information on linkage across many genomic markers from three hybrid crosses, we

anchor the draft genome assembly to pseudomolecules and estimate the landscape of recombination across the genome. Finally, using an additional map that integrates the amplified fragment length polymorphism (AFLP) markers from previous QTL studies in *L. kohalensis* and *L. paranigra*, we approximate the location of known male song QTL, including one co-localizing with a female acoustic preference QTL, on the pseudomolecules. We examine local variation in recombination rates across the genome and in relation to the location of the song and preference QTL to test the hypothesis that song-preference co-evolution is facilitated by suppressed interspecific recombination. This study provides important insight into the role of the genomic architecture during divergence of closely related species separated by premating barriers.

MATERIAL & METHODS

De novo genome assembly

The *Laupala kohalensis* draft genome (estimated genome size ~ 1.9 Gb; Petrov *et al.* 2000) was sequenced using the Illumina HiSeq 2500 platform. DNA was isolated with the DNeasy Blood & Tissue Kits (Qiagen Inc., Valencia, CA, USA) from six immature female crickets (c. five months of age) chosen randomly from a laboratory stock population (approximate lab generation=14). Females were chosen to balance DNA content of sex chromosomes to autosomes (female crickets are XX; male crickets are XO). DNA was subsequently pooled for sequencing. Four different libraries were created: a paired-end library with an estimated insert size of 200 bp (sequenced by Cornell Biotechnology Resource Center), a paired-end library with an estimated insert size of 500 bp, and two mate-pair libraries with insert sizes of 2 and 5 Kb (sequenced by Cornell Weill College Genomics Resources Core Facility).

Reads were processed using Fastq-mcf from the Ea-Utils package (Aronesty 2011) with the parameters -q 30 (trim nucleotides from the extremes of the read with qscore below 30) and -l 50 (discard reads with lengths below 50 bp). Read duplications were removed using PrinSeq (Schmieder and Edwards 2011) and reads were corrected using Musket with the default parameters (Liu *et al.* 2013).

Reads were assembled using SoapDeNovo2 (Luo *et al.* 2012). The reads were assembled using different Kmer sizes (k = 31, 39, 47, 55, 63, 71, 79 and 87). The 87-mer assembly produced the best assembly (based on N50/L50, assembly size, and number of scaffolds). Scaffolds and contigs were renamed using an in-house Perl script. Gaps were filled using GapCloser from the SoapDeNovo2 package.

The gene space covered by the assembly was evaluated using three different approaches. (1) *Laupala kohalensis* unigenes produced by the Gene Index initiative (Cricket release 2.0: http://compbio.dfci.harvard.edu/cgi-bin/tgi/gimain.pl?gudb=cricket) were mapped using Blat (Kent 2002). Only unigenes mapping with 90% or more of their length were considered; (2) 50 bp paired-end RNA-seq reads from a congeneric species, *L. cerasina* were mapped using Tophat2 (Kim *et al.* 2013). Reads were processed using the same methodology described above, but using a minimum length of 30 bp; (3) using BUSCO (Simão *et al.* 2015) to search for conserved eukaryotic and arthropod genes.

Samples

We generated three F_2 interspecies hybrid families to estimate genetic maps. Multiple F_1 male and sibling females were intercrossed to generate F_2 mapping populations for the following species crosses: (1) a *L. kohalensis* female and *L. paranigra* male (“ParKoh”, 178 genotyped F_2

hybrid offspring; previously reported in Shaw et al. 2007); (2) a *L. kohlanesis* female and a *L. pruna* male ("PruKoh", 193 genotyped F_2 hybrid offspring); (3) a *L. paranigra* female and a *L. kona* male ("KonPar", 263 genotyped F_2 hybrid offspring). These four species are part of a recently radiated clade showing conspicuous mating song divergence (Mendelson and Shaw 2005). Approximate geographic distributions of the species, phylogenetic relationships and parent collection localities are shown in Fig 1 and in Table S1. Crickets used in crosses were a combination of lab stock and outbred individuals (*L. kohalensis* [for ParKoh] and *L. paranigra* [for ParKoh and KonPar] were both lab reared for 3-15 generations; *L. kohalensis* [for PruKoh], *L. pruna* and *L. kona* were wild-caught). All parental and hybrid generations were reared in a temperature-controlled room (20°C) on Purina cricket chow and provided water *ad libitum*.

Genotyping

DNA was extracted from whole adults using the DNeasy Blood & Tissue Kits (Qiagen, Valencia, CA, USA). Genotype-by-Sequencing library preparation and sequencing were done in 2014 at the Genomic Diversity Facility at Cornell University following Elshire *et al.* (2011). The Pst I restriction enzyme was used for sequence digestion and DNA was sequenced on the Illumina HiSeq 2500 platform (Illumina Inc., USA).

Reads were trimmed and demultiplexed using Flexbar (Dodt *et al.* 2012) and then mapped to the *L. kohalensis de novo* draft genome using Bowtie2 (Langmead and Salzberg 2012) with default parameters. We then called SNPs using two different pipelines: The Genome Analysis Toolkit (GATK; DePristo *et al.* 2011; Van der Auwera *et al.* 2013) and FreeBayes (Garrison and Marth 2012). For GATK we used individual BAM files to generate gVCF files using 'HaplotypeCaller' followed by the joint genotyping step 'GenotypeGVCF'. We then evaluated variation in SNP quality across all genotypes using custom R scripts to determine appropriate settings for hard

filtering based on the following metrics (based on the recommendations for hard filtering section "Understanding and adapting the generic hard-filtering recommendations" at https://software.broadinstitute.org/gatk/ accessed on 28 February 2017): quality-by-depth, Phred-scaled *P*-value using Fisher's Exact Test to detect strand bias, root mean square of the mapping quality of the reads, u-based z-approximation from the Mann-Whitney Rank Sum Test for mapping qualities, u-based z-approximation from the Mann-Whitney Rank Sum Test for the distance from the end of the read for reads with the alternate allele. For FreeBayes we called variants from a merged BAM file using standard filters. After variant calling we filtered the SNPs using 'vcffilter', a Perl library part of the VCFtools package (Danecek *et al.* 2011) based on the following metrics: quality (> 30), depth of coverage (> 10), and strand bias for the alternative and reference alleles (SAP and SRP, both > 0.0001). Finally, the variant files from the GATK pipeline and the FreeBayes pipeline were filtered to only contain biallelic SNPs with less than 10% missing genotypes using VCFtools.

We retained two final variant sets: a high-confidence set including only SNPs with identical genotype calls between the two variant discovery pipelines and the full set of SNPs which included all variants called using FreeBayes but limited to positions that were shared among the GATK and FreeBayes pipelines.

Linkage mapping

The genotype information from the parental lines was used to assign ancestry to the SNP loci. The parents of the crosses were heterogeneously heterozygous and only ancestry informative loci were retained, i.e. all loci for which one or more of the parents was heterozygous were discarded. We were unable to obtain sequence data from the parents for PruKoh, but used sequence data from a single, non-parental *L. pruna* female, and three available *L. kohalensis* females, all from

the same populations as the parents. Ancestry was inferred if all three *L. kohalensis* individuals were homozygous for one allele and the *L. pruna* individual was homozygous for the alternative allele. All other loci were discarded. The loci were then further filtered based on genotype similarity and segregation distortion (see below for details).

The linkage maps deriving from the three species crosses were generated independently and by taking a three-step approach, employing both the regression mapping and the maximum likelihood (ML) mapping functions in JoinMap 4.0 (van Ooijen 2006) as well as the three-point error-corrected ML mapping function in MapMaker 3.0 (Lander *et al.* 1987; Lincoln *et al.* 1993).

In the first step, we estimated "initial" maps that are relatively low resolution (5 cM) but with high marker order certainty. For initial maps, we first grouped ($3.0 \leq LOD \leq 5.0$) and then ordered the high-confidence markers that showed no segregation distortion (markers with χ^2-square associated *P*-value for deviation from Mendelian inheritance < 0.05 were discarded) and for which no marker had more than 95% similarity in genotypes across individuals compared to other markers (otherwise, one of each pair was excluded). When excluding similar loci, we favored those marker loci shared among the three mapping populations over markers unique to one or two crosses. We then checked for concordance among the three mapping algorithms. In most cases, the maps were highly concordant (in ordering of the markers; with respect to cM among markers, distances differed depending on the algorithm, especially between the regression and ML methods in JoinMap). Discrepancies among the maps produced by the different algorithms for the same cross were resolved by optimizing the likelihood and total length of a given map as well as by using the information in JoinMap's "Genotype Probabilities" and "Plausible Positions".

These initial maps were then filled out using MapMaker with marker loci passing slightly more lenient criteria: markers drawn from the full set of SNPs, with false discovery rate (Benjamini and Hochberg 1995) corrected *P* value for χ^2- square test of deviation from Mendelian inheritance ≤ 0.05 and fewer than 99% of their genotypes in common with other markers loci. First, more informative markers (no missing genotypes, > 2.0 cM distance from other markers) were added satisfying a log-likelihood threshold of 4.0 for the positioning of the marker (i.e., assigned marker position is 10,000 times more likely than any other position in the map). Remaining markers were added at the same threshold, followed by a second round for all markers at a log-likelihood threshold of 3.0. We then used the ripple algorithm on 5-marker windows and explored alternative orders.

In the second step, "comprehensive" maps were obtained in MapMaker by sequentially adding markers from the full set of SNPs that met the more lenient criteria described above to the initial map. Markers were added if they satisfied a log-likelihood threshold of 2.0 for the marker positions, followed by a second round with a log-likelihood threshold of 1.0. We then used the ripple algorithm again on 5-marker windows and explored alternative orders. Typically, MapMaker successfully juxtaposes SNP markers from the same scaffold. However, in marker dense regions with low recombination rates, the likelihoods of alternative marker orders coalesce. In such regions, when multiple markers from the same genomic scaffold were interspersed by markers from a different scaffold, we repositioned the former markers by forcing them in the map together. If the log-likelihood of the map decreased by more than 3.0 (factor 1000), only one of the markers from that scaffold was used in the map. The comprehensive maps provide a balance between marker density and confidence in marker ordering and spacing.

294 The third step was to create "dense" maps. We added all remaining markers that were not
295 yet incorporated in step two, first at a log-likelihood threshold of 0.5, followed by another round
296 at a log-likelihood threshold of 0.1. We then used the ripple command as described above. The
297 dense maps are useful for anchoring of scaffolds and for obtaining the highest possible resolution
298 of variation in recombination rates, but with the caveat that there is some uncertainty in marker
299 order. Uncertainty is expected to be higher towards the centers of the linkage groups where
300 crossing over events between adjacent markers become substantially less frequent (see Results).

301 *Comparative analyses*

302 Based on the recent divergence times and high interbreeding successes, we predict a large degree
303 of collinearity of the linkage maps. We note that interpretations must take into account the non-
304 independence of the ParKoh and PruKoh/KonPar maps, as only comparing PruKoh and KonPar
305 comprises a fully independent contrast. We first examined whether inversions or other
306 chromosomal rearrangements were common (affecting linkage map lengths and marker orders)
307 or whether maps were generally collinear by comparing among the initial and comprehensive
308 linkage maps visually using map graphs from MapChart (Voorrips 2002). Inverted or transposed
309 markers present in two or all maps can be detected by connecting "homologs" in MapChart (a
310 homolog in this case means a scaffold that is represented in two or more maps). Then, we tested
311 whether linkage maps are generally collinear across the species pairs quantitatively. We used
312 Spearman's rank order correlation (ρ) test to examine the strength of correlation between the
313 order in shared markers (the homologs in MapChart). We calculated ρ and the corresponding *P*-
314 value (the probability of observing the measured or stronger correlation given no true correlation
315 exists) by using the cor.test() function in R (R Development Core Team 2016).

316 We then tested for genetic incompatibilities among the genomes of the four species, by
317 measuring segregation distortion in sliding, 10 cM windows. Although we filtered out markers
318 with very high levels of segregation distortion (using a 5% FDR cutoff) to purge markers with
319 potential sequencing errors, groups of distorted markers in a single region of a linkage group
320 represent genomic regions with biased parental allele contributions, suggesting genetic
321 incompatibilities (or, less common, selfish alleles and other active segregation distorters).
322 Because *L. kohalensis* and *L. paranigra* are more distantly related to each other (and, thus,
323 allowing more time for genetic incompatibilities to accumulate) than they are to *L. pruna* and *L.*
324 *kona*, respectively (Mendelson and Shaw 2005; see Fig 1.), we expected more regions with
325 significant segregation distortion in the ParKoh map relative to the KonPar and PruKoh maps.
326 We calculated genotype frequency and the negative 10-base logarithm of the *P* value for the χ^2-
327 square test of deviation from Mendelian inheritance across the linkage groups in R using the
328 R/qtl package (Broman *et al.* 2003). Windows with $P < 0.01$ were considered to have significant
329 segregation distortion, und thus potentially reflecting genetic incompatibilities.

330 After establishing that the linkage maps were generally collinear (see Results), we merged the
331 maps and examined patterns of variation in crossing over along the *Laupala* genome. Maps were
332 consolidated using ALLMAPS (Tang *et al.* 2015). Then, we calculated species-specific average
333 recombination rates for the linkage groups by dividing the total length of the linkage group (in
334 cM) by the physical length of the pseudomolecule (in million bases, Mb) obtained by merging
335 homologous linkage groups using ALLMAPS. Lastly, to evaluate recombination rate variation
336 along the linkage groups, we fitted smoothing splines (with 10 degrees of freedom, based on the
337 fit of the spline to the observed data) in R to describe the relationship between the consensus
338 physical distance (as per the anchored scaffolds) and the genetic distance specific to each linkage

map. Variation in the recombination rate was then assessed by taking the first derivative (i.e. the rate) of the fitted spline function. The estimated recombination rates are likely to be an overestimate of the true recombination rate, because unplaced/unordered parts of the assembly do not contribute to the physical length of the pseudomolecules but are reflected in the genetic distances obtained from crossing-over events in the recombining hybrids.

To test the hypothesis that linked trait and preference genes reside in low recombination regions, we integrated the AFLP map and song and preference QTL peaks identified in previous work on *L. kohalensis* and *L. paranigra* (Shaw and Lesnick 2009) with the current ParKoh SNP map and projected the QTL peaks onto the anchored genome. The SNPs used in the present study were obtained from the same mapping population (same individuals) as in the 2009 AFLP study. Therefore, we combined the high confidence SNPs described above (for the "initial" map) with the AFLP markers reported in (Shaw *et al.* 2007) that were of the same individuals as the SNP markers used in this study and created a new linkage map using the same stringent criteria as for the "initial" maps described above. We projected this map onto the anchored draft genome based on common markers (scaffolds). We then approximated the physical location of the QTL peaks by looking for SNP markers on scaffolds present in the draft genome flanking AFPL markers underneath the QTL peaks identified in the 2009 study.

DATA ACCESIBILITY

Supplementary files are available on FigShare. See section "supplementary materials" for details. Raw data (vcf files, linkage maps, pseudomolecule agp file), and R-scripts will be deposited on FigShare after final acceptance and are available upon request. The genome assembly and sequencing reads are available on NCBI's GenBank under BioProject number PRJNA392944.

The Genotype-by-sequencing reads will be made available in NCBI's short read archive under BioProject number PRJNA429815

RESULTS

De novo genome assembly

The sequencing of the four libraries yielded 162.5 Gb of raw sequences (Table 1). After read processing, 145.5 Gb was used for the sequence assembly. We compared among assemblies resulting from different Kmer sizes (k = 31, 39, 47, 55, 63, 71, 79 and 87). Based on the N50/L50 and the total assembly size, the assembly produced with k = 87 was retained for the final draft genome. Despite a large number of scaffolds in the final assembly (149,424), the median length of the scaffolds was high and the total length of the assembly covers about 83% of the expected complete genome in *Laupala*.

Gene space coverage in the assembly was evaluated using the *L. kohalensis* cricket gene index (Danley *et al.* 2007) (release 2.0), RNASeq from *Laupala cerasina* (Blankers *et al.* 2018), and by performing a BUSCO search using eukaryotic and arthropod specific conserved genes. Respectively 95% and 92% of the *Laupala* gene index and RNAseq sequences mapped to the current genome. In addition, the BUSCO search indicated very few missing genes in either database (Table 1).

Table 1. *Laupala kohalensis* sequencing, assembly and gene space evaluation statistics.

Sequencing Statistics	**Raw data**		**Processed data**	
Library	**Size (Gb)**	**Coverage[a]**	**Size (Gb)**	**Coverage[a]**
Paired End 0.2 Kb inserts	28.9	15	26.1	14

Paired End 0.5 Kb inserts	63.1	33	59.8	31
Mate Pair 2 Kb inserts	36.2	19	31.8	17
Mate Pair 5 Kb inserts	34.3	18	27.8	14
Total	162.5	85	145.5	76

Assembly Statistics	**Contigs**	**Scaffolds**
Total assembly size (Gb)	1.6	1.6
Total assembled sequences	219,073	148,874
Longest sequence length (Kb)	465	4,541
Average sequence length (Kb)	7.2	10.7
N90 index[b]	40,926	3,505
N90 length (Kb)	7.7	67.7
N50 index	9,917	756
N50 length (Kb)	43.6	583
GC content (%)	34.9%	34.9%

Gene Space Statistics	**Mapping percentage**
Laupala unigenes from the Gene Index	95%
Laupala RNASeq reads	92%

BUSCO database	Complete	Single copy	Duplicated	Fragmented	Missing	Total
Eukaryota_odb9	98.7%	93.7%	5.0%	0.3%	1.0%	303
Arthropoda_odb9	99.3%	96.8%	2.5%	0.1%	0.6%	1066

[a]Coverage is based in an estimated genome size of 1.91 Gb (Petrov *et al.* 2000)

[b]When ordering all contigs (or scaffolds) by size, the N50 or N90 index indicates the number of the longest sequences (contigs or scaffolds) that contain 50% or 90%, respectively, of the total assembled sequence. The N50 and N90 length indicate the length of the shortest sequence in the set of the largest contigs (or scaffolds) that contain 50% or 90%, respectively, of all the sequence in the assembly.

Collinear linkage maps

We obtained 815,109,126; 522,378,849; and 311,558,401 reads after demultiplexing for ParKoh, KonPar, and PruKoh, respectively. Average sequencing depth ± standard deviation across all

391 individuals in the F2 mapping population after filtering, (before and) after marker selection based
392 on segregation distortion and ancestry information for linkage mapping was (62.4 x ± 162.5)
393 52.2 x ± 31.4, (44.3 x ± 58.5) 38.1 x ± 23.8, and (56.1 x ± 105.7) 41.8 x ± 29.3, respectively.

394 In the initial maps, 158 (ParKoh), 170 (KonPar), and 138 (PruKoh) markers were grouped into
395 eight linkage groups at a LOD score of 5.0, corresponding to the seven autosomes and one X-
396 chromosome in *Laupala.* The corresponding marker spacing was 5.14, 4.85, and 7.33 cM. The
397 comprehensive maps contained 526, 650, and 325 markers with an average marker spacing of
398 1.91, 1.37, and 3.25 cM and on the dense maps we placed 608, 823, and 383 markers with on
399 average 1.69, 1.37, and 3.25 cM. between markers

400 The recent divergence times and the limited levels of post-zygotic isolation observed in this
401 system led us to hypothesize that the linkage maps would show a high degree of collinearity. The
402 visual comparison of marker positioning showed that the relative locations of shared scaffolds
403 were similar across the linkage maps in both the initial and the comprehensive maps (Fig 2, Fig
404 S1). However, we also observe substantial variation in the total genetic length of homologous
405 linkage groups, indicating recombination rate variation (Fig 2, Fig S1). This variation may in
406 part result from chromosomal rearrangements. However, we can only reliably detect
407 rearrangements in our maps if they are not segregating within species *and* are fixed for
408 alternative arrangements between *L. pruna* and *L. kohalensis* on the one side and *L. paranigra*
409 and *L. kona* on the other side. In that specific scenario the inverted marker order is visible when
410 contrasting the PruKoh and KonPar maps, while the ParKoh map would show reduced
411 recombination in that area (Fig 1C). Despite the apparent variation in recombination rates among
412 homologous linkage groups, Spearman's rank correlation of pairwise linkage group comparisons
413 was high (ρ varied between 0.91 and 1.00) and similar to values seen in comparisons of

intraspecific linkage maps (e.g. Poursarebani *et al.* 2013); the quantitative measure of collinearity was largely consistent across linkage groups and across cross types (Table 2). Finally, merging the maps into a consensus pseudomolecule assembly allowed us to measure the error between individual maps and the merged assembly. Correlations between linkage maps and the pseudomolecule assembly were generally high (> 0.95), indicating substantial synteny (Fig S2).

Table 2. Linkage map comparison. Spearman's rank correlation (ρ) is shown for each pairwise comparison of linkage maps across all 8 linkage groups.

	ParKoh ~ KonPar	ParKoh ~ PruKoh	KonPar ~PruKoh
1	0.99‡	0.90‡	0.97‡
2	0.99‡	0.96‡	0.93‡
3	1.00‡	0.98‡	0.95‡
4	0.99‡	1.00‡	0.97‡
5	0.97‡	0.98‡	0.95‡
6	0.99‡	0.94‡	0.94‡
7	0.96‡	0.93†	0.91‡
X	0.92‡	0.96‡	0.99‡

* $P < 0.01$; † $P < 0.001$; ‡ $P < 0.0001$

Limited heterogeneity in segregation distortion

We expected genetic incompatibilities to be more likely to occur in the ParKoh cross than in the KonPar and PruKoh cross, because *L. kohalensis* and *L. paranigra* are more distantly related than any of the other species pairs (Fig 1). We tested this hypothesis by examining the degree of segregation distortion in markers within 10 cM sliding windows across the linkage maps. Overall, segregation distortion was limited and average genotype frequencies were close to

Mendelian expectations (Fig 3). However, LG3 showed a bias against *L. kohalensis* homozygotes in the ParKoh cross but not in any of the other crosses. Additionally, there was significant variation in the frequency of heterozygotes across the linkage groups (linear model Freq[heterozygotes]~LG x cross: $R^2 = 0.21$, $F_{20,1547} = 20.7$, $P < 0.0001$). Post-hoc Tukey Honest Significant Differences revealed that linkage group 7 had the lowest abundance of heterozygotes overall and within each of the intercrosses and that levels of heterozygosity on LG 7 were similar across the maps (Table S2). Together, these results show that from some LGs and in some crosses, certain genotype combinations were less common than expected, potentially as a result for genetic incompatibilities or meiotic drive.

Variable recombination rates across the genome

We anchored a total of 1054 scaffolds covering 720 million base pairs, a little below half the current genome assembly (see Table S3 for scaffold number, N50, and assembly size per LG and Fig S3 for coverage variation across the linkage groups). This gives us enough power to make inferences about broad-scale recombination rate variation, but not about the existence of small-scale recombination hotspots. Average recombination rates (cM/Mb) varied from between 0.75 (KonPar) and 0.93 (ParKoh) on the X chromosome to between 3.12 (KonPar) and 4.24 (PruKoh) on LG6 (Table 3). We note that the recombination rate for LG6 might be artificially inflated because of lower assembly quality (expressed as N50) of this LG relative to the other LGs in all linkage maps and in the pseudochromosomes (Table S3). Both including and excluding the sex chromosome, there is a significant linear relationship between chromosome size and genetic length (linear mixed effect model with cross as random variable; With X: $\beta = 0.62$, $F_{1,23} = 14.95$, $P = 0.0008$; without X: $\beta = 0.69$, $F_{1,20} = 29.7$, $P < 0.0001$) and between chromosome size and

broad-scale recombination rate (with X: β = -34.1, $F_{1,23}$ = 29.1, $P < 0.0001$).; without X: β = -24.0, $F_{1,23}$ = 63.7, $P < 0.0001$).

Table 3. Linkage map summary statistics.

LG	Length (Mb)	ParKoh Map length (cM)	ParKoh Rec. Rate (cM/Mb)	KonPar Map length (cM)	KonPar Rec. Rate (cM/Mb)	PruKoh Map length (cM)	PruKoh Rec. Rate (cM/Mb)
1	117	207	1.77	156	1.33	156	1.33
2	102	167	1.64	128	1.25	205	2.01
3	137	169	1.23	167	1.22	173	1.26
4	90	100	1.11	117	1.30	99	1.10
5	62	91	1.47	84	1.35	103	1.66
6	25	85	3.40	106	4.24	78	3.12
7	53	78	1.47	84	1.58	139	2.62
X	134	124	0.93	101	0.75	114	0.85
Total	**720**	**1021**	**1.42**	**943**	**1.31**	**1067**	**1.48**

Most linkage groups showed wide regions of strongly reduced recombination rates in the center of the linkage groups (Fig. 4). The general pattern of peripheral peaks in recombination rates juxtaposing large recombination "desserts" was similar among the three intercrosses, but some additional cross-specific peaks in recombination rates were observed on almost all linkage groups (Fig 4).

Trait-preference co-evolution despite high recombination

Contrary to our expectation, the approximate location of the colocalizing song and preference QTL peak from (Shaw and Lesnick 2009) was associated with average recombination rates in the ParKoh and KonPar map and low recombination rates in the PruKoh map (Fig 4; Table S4). However, most other QTL peaks are located in regions of low recombination (Fig 4; Table S4).

DISCUSSION

The evolutionary trajectory of diverging populations and the likelihood of speciation can be heavily influenced by recombination. Within species, recombination can create favorable combinations of alleles or decouple deleterious from beneficial alleles. Among species, regions with low recombination can provide a genetic shield against introgression of maladaptive loci (Noor *et al.* 2001; Rieseberg 2001; Butlin 2005; Slatkin 2008; Noor and Bennett 2009; Cutter and Payseur 2013; Ortiz-Barrientos *et al.* 2016). Understanding recombination is thus critical to understanding adaptation and speciation. Recombination also has important implications for the analysis of genotype-phenotype relationships (Mackay 2001), demographic inference (Li and Durbin 2011), and analyses of genomic variation (Cutter and Payseur 2013; Wolf and Ellegren 2016). However, we still have limited insight into the patterns of recombination rate variation among species and across genomes, in particular for radiations powered largely by behavioral isolation.

Here, we study four species of sexually divergent Hawaiian swordtail crickets and generate the first pseudomolecule-level assembly for Orthoptera and the first published genome assembly for crickets, an important model system in neurobiology, behavioral ecology, and evolutionary genetics (Horch *et al.* 2017). Below, we discuss how our results provide insight into the potential for structural variation (linkage map collinearity) and genetic incompatibilities to drive reproductive isolation among closely related *Laupala* species. We also elaborate on the patterns of variation in recombination rates across the genome. We then discuss the surprising finding that colocalizing male song and female preference QTL did not fall in a region with particularly low recombination. This is important because it challenges the hypothesis that co-evolution of traits and preferences is facilitated by locally reduced recombination between recently diverged populations.

Collinearity of Genetic Maps

Based on the recent divergence (Mendelson and Shaw 2005) and strong premating isolation of *Laupala* species in the absence of conspicuous morphological and ecological differences (Otte 1994; Shaw 1996; Mendelson and Shaw 2005), we expected limited variation in chromosome structure and few signatures of genetic incompatibility between the species. In line with these expectations, we found that linkage groups are collinear across interspecies crosses (Fig 2). This was true both for comparisons of non-independent species pairs (between ParKoh and the other two crosses), as well as for the independent contrast of the PruKoh map versus the KonPar map. We saw some instances where markers occupied regions that may have been translocated or inverted. However, these instances were rare (Fig 2, Fig S1) and recombination rates were similar among homologous linkage groups across the hybrid families (Fig 4). Moreover, quantitative measures of correlation (Spearman's rank correlation among maps, Pearson's correlation coefficient between maps and the pseudomolecule assembly) as well as limited segregation distortion (but see discussion of one exception below) both supported the collinearity hypothesis.

Variation in the organization and structure of chromosomes can contribute to postzygotic reproductive isolation after speciation as well as to the speciation process directly (Noor *et al.* 2001; Rieseberg 2001). We conclude that at least for the *Laupala* group that radiated on the Big Island of Hawaii in the last 500,000 years, structural rearrangements have not played a major role in the evolution of reproductive isolation. This is because, similar to two hybridizing *Heliconius* species (Davey *et al.* 2017), we observed that chromosome-wide recombination rates are relatively conserved and large chromosomal rearrangements are absent. We hypothesize that for *Laupala* on the Big Island premating isolation combined with (partial) geographic separation

513 (i.e. low migration rates) provides a sufficiently strong barrier to gene flow between sister
514 species. Indeed, as has been shown in recent models of the role of inversions in speciation,
515 genomic rearrangements can only invade and spread in diverging populations if levels of gene
516 flow and the contribution of structural variation to isolation (by linking adaptive alleles or
517 incompatibilities) is high relative to the strength of assortative mating (Feder *et al.* 2014; Dagilis
518 and Kirkpatrick 2016).

519 We acknowledge that the power to detect rearrangements and changes in recombination rates is
520 limited by the resolution of our maps. The average spacing of markers is between 1.37 and 3.25
521 cM. Thus, the upper limit of the magnitude of intervals within which we can detect
522 rearrangements is on the order of 10^5 and 10^6 bp. Due to constraints on the sample size and
523 sequencing strategy, it is thus difficult to attribute subtle variation in marker order and genetic
524 distance between the maps to genomic rearrangements versus mapping errors and sampling
525 variance. Closely related organisms typically show conserved recombination rates within 500 kb
526 intervals; more heterogeneity might be revealed at higher resolution (Stevison *et al.* 2017).

527 *Genetic incompatibilities*

528 We expected genetic incompatibilities to be more likely between genomes of more distantly
529 related species. Accordingly, we discovered a single region covering approximately half of
530 linkage group 3 with high segregation distortion in ParKoh; we found no such deviations in the
531 other two crosses (Fig 3). Inspection of genotype frequencies indicated that there were fewer
532 individuals than expected that were homozygous for *L. kohalensis* alleles for loci in this region.
533 In a controlled cross, segregation distortion can be caused by prezygotic effects such as meiotic
534 drive of selfish genetic elements and distorter genes (e.g. like *sd* in *Drosophila melanogaster*
535 (Larracuente and Presgraves 2012)), and by postzygotic genetic incompatibilities (Dobzhansky

1937; Muller 1942; Burt and Trivers 2006; Presgraves 2010; Hallmann *et al.* 2017). Genotypic errors may produce superficially similar patterns but are unlikely to distort segregation over large genomic regions and with consistent bias towards the same genotypes. Although meiotic drive is a possible alternative to genetic incompatibilities, we do not see the same effect in the other cross involving *L. paranigra*, where selfish genetic elements or segregation distorters ought to have a similar effect. Overall, the large region on linkage group 3 reveals a potential local post-mating barrier to gene flow that could contribute to strengthening existing prezygotic barriers in secondary contact zones or following episodes of migration.

Recombination landscape

Chromosomal rearrangements influence genomic divergence by locally altering recombination rates within and among species. Felsenstein (1974, 1981) illuminated the role of *intraspecific* recombination in purging deleterious alleles and the role of *interspecific* recombination in decoupling co-adapted alleles. In recent years, the role of recombination and its interaction with divergent selection and adaptation on genomic scales have received considerable attention (e.g. Yeaman and Whitlock 2011; Feder *et al.* 2012; Samuk *et al.* 2017) and technological advances are shifting focus towards characterizing the recombination landscape across species (Butlin 2005; Slatkin 2008; Noor and Bennett 2009; Barb *et al.* 2014; Burri *et al.* 2015).

Here, we show that there is limited variation in recombination rates across the maps of three interspecific crosses (Fig 4), but strong heterogeneity in recombination rates across the genome. Genome-wide average interspecific recombination rate varied between 1.3 and 1.5 cM/Mb (Table 3), similar to intraspecific rates observed in dipterans and substantially lower than social hymenopterans and lepidopterans (Wilfert *et al.* 2007). We note that our estimates are derived from interspecific maps, which may lead to somewhat lower estimates compared to intraspecific

559 maps (e.g. Beukeboom *et al.* 2010), where genetic incompatibilities and rearrangements may
560 reduce rates of crossing over; however, differences between intra and interspecific recombination
561 might be negligible if rearrangements are rare (e.g., Davey *et al.* 2017). Moreover, we anchored
562 about 50% of the nucleotides in the draft assembly to linkage groups, and there remain many
563 scaffolds not mapped to a genomic position. These 'missing' scaffolds are expected to add to the
564 physical length of the chromosomes more so than to the genetic length of the chromosomes, thus
565 lowering the recombination rate. However, our study emphasized relative patterns of
566 recombination, which should not be affected by our sampling. And while we can only
567 approximate intraspecific recombination rates at this point, we note that recent divergence of the
568 species involved and collinearity of the linkage maps support conservation of recombination
569 landscapes across intraspecific and interspecific comparisons.

570 Interestingly, for all three species pairs we document high variability in interspecific
571 recombination across genomic regions. We found large regions of low recombination in all three
572 maps, with recombination rates well below 1 cM/Mb and occasionally approaching zero, flanked
573 by steep inclines reaching rates up to 6 cM/Mb (Fig 4). This pattern is consistent with earlier
574 findings in plants (Anderson *et al.* 2003), invertebrates (Rockman and Kruglyak 2009; Niehuis *et*
575 *al.* 2010), and vertebrates (Backström *et al.* 2010; Roesti *et al.* 2013; Singhal *et al.* 2015), but
576 differs from observations in, for example, *Drosophila* (Kulathinal *et al.* 2008) and humans
577 (Myers *et al.* 2005), that show heterogeneity in recombination rates, but not necessarily much
578 higher rates on the periphery of the chromosomes. Commonly invoked drivers of local
579 recombination suppression, such as selection against recombination due to negative epistasis or
580 the maintenance of linkage disequilibrium between mutually beneficial alleles (Smukowski and
581 Noor 2011; Stevison *et al.* 2011; Smukowski Heil *et al.* 2015; Ortiz-Barrientos *et al.* 2016), are

582 not likely to leave chromosome wide signatures. Rather, the observed pattern is more likely
583 attributable to structural properties of chromosomes, such as the location of the centromere and
584 heterochromatin-rich regions (Copenhaver *et al.* 1999; Haupt *et al.* 2001). Roesti *et al*. (2013)
585 observe similar recombination landscapes in stickleback and suggest it might be due to
586 peripheral clustering during meiosis prophase I to facilitate homolog pairing (Harper *et al.* 2004;
587 Brown *et al.* 2005). Regardless of the mechanism, the observed genomic architecture will drive
588 substantial heterogeneity in the propensity of favorable and/or maladaptive alleles to come
589 together, break apart, and introgress in heterospecific backgrounds.

590 *Trait-Preference Co-evolution*

591 On way in which recombination heterogeneity may be important in the study system is in
592 facilitating trait-preference co-evolution. If trait and preference genes are coupled through
593 physical linkage (Kirkpatrick and Hall 2004), linkage can be stronger and span wider physical
594 distances in regions with reduced recombination. We hypothesized that recombination facilitates
595 linkage between trait and preference genes in *Laupala* because a previous study showed that a
596 major song QTL (~ 9% of the parental difference in male song) co-localizes with a preference
597 QTL (~14% of parental difference for female preference) in a cross between *L. kohalensis* and *L.*
598 *paranigra* (Shaw and Lesnick 2009). Contrary to our expectation, we show that the co-localizing
599 QTL fall in a region with intermediate to high recombination rates (> 2.0 cM) compared to
600 chromosomal averages (typically 1 - 2 cM). This suggests that reduced recombination over larger
601 physical distances is unlikely to be driving trait-preference co-evolution in this system.
602 Importantly, a high speciation rate and wide-spread divergence in sexual signaling phenotypes
603 suggest a primary role for trait-preference co-evolution in *Laupala* speciation (Mendelson and
604 Shaw 2005; Shaw *et al.* 2011). Additionally, although these species have likely diverged in

allopatry (Mendelson and Shaw 2005), some level of interspecific gene exchange is likely given historical biogeography, widespread secondary contact and evidence derived from discordant nuclear and mitochondrial gene trees (Shaw 2002).

How then is linkage disequilibrium between traits and preferences maintained? First, QTL may co-localize due to very tight physical linkage or pleiotropy instead of looser linkage. Under these two mechanisms, a lack of physical space for crossing over to occur rather than low recombination rates maintains linkage disequilibrium. Linkage disequilibrium might also persist in the face of recombination if strong assortative mating results from female mate preference. In this case, genetic correlations between the sexes will evolve, coupling signal and preference independent of their genetic distance (Fisher 1930; Lande 1981). Recent simulation studies showed that the probability with which recombination rate modifiers that link co-adaptive alleles spread in a populations is lower when assortative mating is strong, recombination between loci is low, and selection on the loci themselves is strong (Feder *et al.* 2014; Dagilis and Kirkpatrick 2016). Third, the current test involves only a single locus and additional tests are required to more robustly examine the relationship between recombination and trait-preference co-evolution. We observed that several known male song QTL on other linkage groups fall in regions of low recombination. Additional female preference QTL covary with these song QTL as well (Wiley *et al.* 2012) although precise map locations are not yet known.

In summary, we find limited variation in chromosome structure among species, but strong heterogeneity in the recombination landscape across the genome. We present a *de novo* genome assembly and anchor a substantial part of the *L. kohalensis* genome to pseudomolecules. Crickets are an important model system for evolutionary and neurobiological research (Horch *et al.* 2017). but limited genomic resources are available. The first Orthopteran pseudomolecule-level

draft genome and recombination rate map are thus important new contributions to future speciation genomics research. This study further provides important insight into the extent to which structural variation and genetic incompatibilities contribute to isolation among closely related, sexually divergent species. We also shine light on the role of recombination in trait-preference co-evolution and argue that current evidence supports that, at least in *Laupala*, the evolution of behavioral isolation is not contingent on structural genomic variation and locally reduced recombination.

ACKNOWLEDGEMENTS

We thank Stephen Chenoweth and two anonymous reviewers for helpful comments that strongly improved the quality of this manuscript. We further thank the Shaw lab, in particular Mingzi Xu, as well as Michael Sheehan and other members from Cornell's Neurobiology and Behavior department for input that contributed to the interpretation of the findings. This work was supported by the National Science Foundation (DEB 1241060, IOS 1257682 and IOS 0843528).

REFERENCES

Anderson L. K., Doyle G. G., Brigham B., Carter J., Hooker K. D., *et al.*, 2003 High-resolution crossover maps for each bivalent of *Zea mays* using recombination nodules. Genetics 165: 849–865.

Andersson M., Simmons L. W., 2006 Sexual selection and mate choice. Trends Ecol. Evol. 21: 296–302.

Arnegard M. E., Kondrashov A. S., Noor M., 2004. Sympatric speciation by sexual selection alone is unlikely. Evolution. 58: 222–237.

649 Aronesty E., 2011 ea-utils: Command-line tools for processing biological sequencing data.
650 Durham, NC : Expr. Anal.

651 Auwera G. A. Van der, Carneiro M. O., Hartl C., Poplin R., Angel G. del, *et al.*, 2013 From
652 FastQ Data to High-Confidence Variant Calls: The Genome Analysis Toolkit Best Practices
653 Pipeline. Curr. Protoc. Bioinformatics 43: 1–11.

654 Backström N., Forstmeier W., Schielzeth H., Mellenius H., Nam K., *et al.*, 2010 The
655 recombination landscape of the zebra finch *Taeniopygia guttata* genome. Genome Res. 20:
656 485–95.

657 Barb J. G., Bowers J. E., Renaut S., Rey J. I., Knapp S. J., *et al.*, 2014 Chromosomal Evolution
658 and Patterns of Introgression in Helianthus. Genetics 197: 969–979.

659 Benjamini Y., Hochberg Y., 1995 Controlling the false discovery rate: a practical and powerful
660 approach to multiple testing. J. R. Stat. Soc. Ser. B 57: 289–300.

661 Beukeboom L. W., Niehuis O., Pannebakker B. A., Koevoets T., Gibson J. D., *et al.*, 2010 A
662 comparison of recombination frequencies in intraspecific versus interspecific mapping
663 populations of Nasonia. Heredity. 104: 302–309.

664 Blankers T., Oh K. P., Shaw K. L., 2018 The genetic basis of inter-island mating behavior
665 divergence. bioRxiv.

666 Broman K. W., Wu H., Sen Ś., Churchill G. A., 2003 R/qtl: QTL mapping in experimental
667 crosses. Bioinformatics 19: 889–890.

668 Brown P. W., Judis L., Chan E. R., Schwartz S., Seftel A., *et al.*, 2005 Meiotic Synapsis
669 Proceeds from a Limited Number of Subtelomeric Sites in the Human Male. Am. J. Hum.

Genet. 77: 556–566.

Bürger R., Akerman A., 2011 The effects of linkage and gene flow on local adaptation: A two-locus continent-island model. Theor. Popul. Biol. 80: 272–288.

Burri R., Nater A., Kawakami T., Mugal C. F., Olason P. I., *et al.*, 2015 Linked selection and recombination rate variation drive the evolution of the genomic landscape of differentiation across the speciation continuum of Ficedula flycatchers. Genome Res. 25: 1656–1665.

Burt A., Trivers R., 2006 Genes in Conflict: The Biology of Selfish Genetic Elements. Belknap, Cambridge, MA.

Butlin R. K., 2005 Recombination and speciation. Mol. Ecol. 14: 2621–2635.

Copenhaver G. P., Nickel K., Kuromori T., Benito M.-I., Kaul S., *et al.*, 1999 Genetic definition and sequence analysis of Arabidopsis centromeres. Science 286: 2468–2474.

Coyne J. A., Orr H. A., 2004 *Speciation*. Sinauer, Sunderland, MA.

Cutter A. D., Payseur B. A., 2013 Genomic signatures of selection at linked sites: unifying the disparity among species. Nat. Rev. Genet. 14: 262–274.

Dagilis A. J., Kirkpatrick M., 2016 Prezygotic isolation, mating preferences, and the evolution of chromosomal inversions. Evolution 70: 1465–1472.

Danecek P., Auton A., Abecasis G., Albers C. A., Banks E., *et al.*, 2011 The variant call format and VCFtools. Bioinformatics 27: 2156–2158.

Danley P. D., Mullen S. P., Liu F., Nene V., Quackenbush J., *et al.*, 2007 A cricket Gene Index: a genomic resource for studying neurobiology, speciation, and molecular evolution. BMC Genomics 8: 109.

691 Davey J. W., Barker S. L., Rastas P. M., Pinharanda A., Martin S. H., *et al.*, 2017 No evidence
692 for maintenance of a sympatric Heliconius species barrier by chromosomal inversions.
693 Evol. Lett. 1: 138–154.

694 DePristo M. A., Banks E., Poplin R., Garimella K. V, Maguire J. R., *et al.*, 2011 A framework
695 for variation discovery and genotyping using next-generation DNA sequencing data. Nat.
696 Genet. 43: 491–498.

697 Dobzhansky T., 1937 *Genetics and the Origin of Species*. Columbia University Press, New York,
698 NY.

699 Dodt M., Roehr J. T., Ahmed R., Dieterich C., 2012 FLEXBAR—flexible barcode and adapter
700 processing for next-generation sequencing platforms. Biology. 1: 895–905.

701 Elshire R. J., Glaubitz J. C., Sun Q., Poland J. A., Kawamoto K., *et al.*, 2011 A robust, simple
702 genotyping-by-sequencing (GBS) approach for high diversity species. PLoS One. 6.

703 Feder J. L., Egan S. P., Nosil P., 2012 The genomics of speciation-with-gene-flow. Trends
704 Genet. 28: 342–350.

705 Feder J. L., Nosil P., Flaxman S. M., 2014 Assessing when chromosomal rearrangements affect
706 the dynamics of speciation: implications from computer simulations. Front. Genet. 5: 295.

707 Felsenstein J., 1981 Skepticism towards Santa Rosalia, or why are there so few kinds of animals?
708 Evolution 35: 124–138.

709 Fisher R. A., 1930 *The genetical theory of natural selection*. Oxford University Press, New
710 York.

711 Garrison E., Marth G., 2012 Haplotype-based variant detection from short-read sequencing.

712 arXiv: 1207.3907.

713 Gavrilets S., 2003 Perspective: models of speciation: what have we learned in 40 years?
714 Evolution 57: 2197–2215.

715 Gillespie J. H., 2000 Genetic drift in an infinite population: the pseudohitchhiking model.
716 Genetics 155: 909–919.

717 Grace J. L., Shaw K. L., 2011 Coevolution of male mating signal and female preference during
718 early lineage divergence of the Hawaiian cricket, Laupala Cerasina. Evolution 65: 2184–
719 2196.

720 Hallmann C. A., Sorg M., Jongejans E., Siepel H., Hofland N., *et al.*, 2017 More than 75 percent
721 decline over 27 years in total flying insect biomass in protected areas. PLoS One 12: 1–21.

722 Harper L., Golubovskaya I., Cande W. Z., 2004 A bouquet of chromosomes. J. Cell Sci. 117:
723 4025-4032.

724 Haupt W., Fischer T. C., Winderl S., Fransz P., Torres-Ruiz R. A., 2001 The centromere1
725 (CEN1) region of Arabidopsis thaliana: architecture and functional impact of chromatin.
726 Plant J. 27: 285–296.

727 Hill W. G., Robertson A., 1966 The effect of linkage on limits to artificial selection. Genet. Res.
728 8: 269–294.

729 Horch H. W., Mito T., Popadic A., Ohuchi H., Noji S. (Eds.), 2017 *The cricket as a model*
730 *organism*. Springer Japan, Tokyo, Japan.

731 Kent W. J., 2002 BLAT—the BLAST-like alignment tool. Genome Res. 12: 656–664.

732 Kim D., Pertea G., Trapnell C., Pimentel H., Kelley R., *et al.*, 2013 TopHat2: accurate alignment

of transcriptomes in the presence of insertions, deletions and gene fusions. Genome Biol. 14: R36.

Kirkpatrick P., 1982 Sexual selection and the evolution of female mate choice. Evolution 36: 1–12.

Kirkpatrick M., Ravigne V., 2002 Speciation by natural and sexual selection: models and experiments. Am. Nat. 159 supple: S22–S35.

Kirkpatrick M., Hall D. W., 2004 Sexual selection and sex linkage. Evolution. 58: 683–691.

Kirkpatrick M., Barton N., 2006 Chromosome inversions, local adaptation and speciation. Genetics 173: 419–434.

Kulathinal R. J., Bennett S. M., Fitzpatrick C. L., Noor M. A. F., 2008 Fine-scale mapping of recombination rate in Drosophila refines its correlation to diversity and divergence. Proc. Natl. Acad. Sci. 105: 10051–10056.

Lande R., 1981 Models of speciation by sexual selection on polygenic traits. Proc Natl Acad Sci 78: 3721–3725.

Lander E., Green P., Abrahamson J., Barlow A., Daly M., *et al.*, 1987 MAPMAKER: An interactive computer package for constructing primary genetic linkage maps of experimental and natural populations. Genomics 1: 174–181.

Langmead B., Salzberg S. L., 2012 Fast gapped-read alignment with Bowtie 2. Nat. Methods 9: 357–359.

Larracuente A. M., Presgraves D. C., 2012 The Selfish Segregation Distorter Gene Complex of Drosophila melanogaster. Genetics 192: 33–53.

754 Li H., Durbin R., 2011 Inference of human population history from individual whole-genome
755 sequences. Nature 475: 493–496.

756 Lincoln S. E., Daly M. J., Lander E. S., 1993 Constructing genetic linkage maps with
757 MAPMAKER/EXP Version 3.0: a tutorial and reference manual. A Whitehead Inst.
758 Biomed. Res. Tech. Rep.: 78–79.

759 Liu Y., Schröder J., Schmidt B., 2013 Musket: a multistage k-mer spectrum-based error corrector
760 for Illumina sequence data. Bioinformatics 29: 308–315.

761 Luo R., Liu B., Xie Y., Li Z., Huang W., *et al.*, 2012 SOAPdenovo2: an empirically improved
762 memory-efficient short-read de novo assembler. Gigascience 1: 18.

763 Mackay T. F. C., 2001 The genetic architecture of quantitative traits. Annu. Rev. Genet. 35:
764 303–339.

765 Marques D. A., Lucek K., Meier J. I., Mwaiko S., Wagner C. E., *et al.*, 2016 Genomics of Rapid
766 Incipient Speciation in Sympatric Threespine Stickleback. PLoS Genet. 12: 1–34.

767 Mendelson T. C., Shaw K. L., 2002 Genetic and behavioral components of the cryptic species
768 boundary between Laupala cerasina and L. kohalensis (Orthoptera: Gryllidae). Genetica
769 116: 301–310.

770 Mendelson T. C., Shaw K. L., 2005 Rapid speciation in an arthropod. Nature 433: 375–376.

771 Muller H., 1942 Isolating mechanisms, evolution, and temperature. Biol. Symp. 6: 71–125.

772 Myers S., Bottolo L., Freeman C., McVean G., Donnelly P., 2005 A Fine-Scale Map of
773 Recombination Rates and Hotspots Across the Human Genome. Science 310: 321–324.

774 Niehuis O., Gibson J. D., Rosenberg M. S., Pannebakker B. A., Koevoets T., *et al.*, 2010

775 Recombination and its impact on the genome of the haplodiploid parasitoid wasp Nasonia.
776 PLoS One 5: e8597.

777 Noor M. A., Grams K. L., Bertucci L. A., Reiland J., 2001 Chromosomal inversions and the
778 reproductive isolation of species. Proc. Natl. Acad. Sci. 98: 12084–8.

779 Noor M. A. F., Bennett S. M., 2009 Islands of speciation or mirages in the desert? Examining the
780 role of restricted recombination in maintaining species. Heredity 103: 439–44.

781 Ooijen J. W. van, 2006 JoinMap 4, Software for the calculation of genetic linkage maps in
782 experimental populations.

783 Ortiz-Barrientos D., Engelstädter J., Rieseberg L. H., 2016 Recombination rate evolution and the
784 origin of species. Trends Ecol. Evol. 31: 226–236.

785 Otte D., 1994 *The Crickets of Hawaii: Origin, Systematics, and Evolution*. Orthoptera
786 Society/Academy of Natural Sciences of Philadelphia, Philadelphia, PA.

787 Otto S. P., 2009 The evolutionary enigma of sex. Am. Nat. 174: S1--S14.

788 Petrov D. A., Sangster T. A., Johnston J. S., Hartl D. L., Shaw K. L., 2000 Evidence for DNA
789 loss as a determinant of genome size. Science 287: 1060–1062.

790 Poursarebani N., Ariyadasa R., Zhou R., Schulte D., Steuernagel B., *et al.*, 2013 Conserved
791 synteny-based anchoring of the barley genome physical map. Funct. Integr. Genomics 13:
792 339–350.

793 Presgraves D. C., 2010 Darwin and the Origin of Interspecific Genetic Incompatibilities. Am.
794 Nat. 176: S45–S60.

795 R Development Core Team R., 2016 R: A Language and Environment for Statistical Computing

(RDC Team, Ed.). R Found. Stat. Comput. 1: 409.

Rieseberg L. H., 2001 Chromosomal rearrangements and speciation. Trends Ecol. Evol. 16: 351–357.

Rockman M. V., Kruglyak L., 2009 Recombinational landscape and population genomics of Caenorhabditis elegans. PLoS Genet 5: e1000419.

Roesti M., Moser D., Berner D., 2013 Recombination in the threespine stickleback genome - Patterns and consequences. Mol. Ecol. 22: 3014–3027.

Samuk K., Owens G. L., Delmore K. E., Miller S. E., Rennison D. J., *et al.*, 2017 Gene flow and selection interact to promote adaptive divergence in regions of low recombination. Mol. Ecol. 26: 4378–4390.

Schmieder R., Edwards R., 2011 Quality control and preprocessing of metagenomic datasets. Bioinformatics 27: 863–864.

Servedio M. R., 2009 The role of linkage disequilibrium in the evolution of premating isolation. Heredity 102: 51–56.

Servedio M. R., Burger R., 2014 The counterintuitive role of sexual selection in species maintenance and speciation. Proc. Natl. Acad. Sci. 111: 8113–8118.

Servedio M. R., 2015 Geography, assortative mating, and the effects of sexual selection on speciation with gene flow. Evol. Appl. 9: 91–102.

Shaw K. L., 1996 Polygenic Inheritance of a Behavioral Phenotype: Interspecific Genetics of Song in the Hawaiian Cricket Genus Laupala. Evolution 50: 256–266.

Shaw K. L., 2000a Further acoustic diversity in Hawaiian forests: two new species of Hawaiian

817 cricket (Orthoptera: Gryllidae: Trigonidiinae: *Laupala*). Zool. J. Linn. Soc. 129: 73–91.

818 Shaw K. L., 2000b Interspecific genetics of mate recognition: inheritance of female acoustic
819 preference in Hawaiian crickets. Evolution 54: 1303–1312.

820 Shaw K. L., 2002 Conflict between nuclear and mitochondrial DNA phylogenies of a recent
821 species radiation: what mtDNA reveals and conceals about modes of speciation in Hawaiian
822 crickets. Proc. Natl. Acad. Sci. 99: 16122–16127.

823 Shaw K. L., Parsons Y. M., Lesnick S. C., 2007 QTL analysis of a rapidly evolving speciation
824 phenotype in the Hawaiian cricket Laupala. Mol. Ecol. 16: 2879–2892.

825 Shaw K. L., Lesnick S. C., 2009 Genomic linkage of male song and female acoustic preference
826 QTL underlying a rapid species radiation. Proc. Natl. Acad. Sci. 106: 9737–9742.

827 Shaw K. L., Ellison C. K., Oh K. P., Wiley C., 2011 Pleiotropy, "sexy" traits, and speciation.
828 Behav. Ecol. 22: 1154–1155.

829 Simão F. A., Waterhouse R. M., Ioannidis P., Kriventseva E. V, Zdobnov E. M., 2015 BUSCO:
830 assessing genome assembly and annotation completeness with single-copy orthologs.
831 Bioinformatics 31: 3210.

832 Singhal S., Leffler E. M., Sannareddy K., Turner I., Venn O., *et al.*, 2015 Stable recombination
833 hotspots in birds. Science 350: 928–932.

834 Slatkin M., 2008 Linkage disequilibrium—understanding the evolutionary past and mapping the
835 medical future. Nat. Rev. Genet. 9: 477–485.

836 Smith J. M., Haigh J., 1974 The hitch-hiking effect of a favourable gene. Genet. Res. 23: 23–35.

837 Smith J. M., 1978 *The Evolution of Sex*. Cambridge University Press Cambridge.

838 Smukowski C. S., Noor M. A. F., 2011 Recombination rate variation in closely related species.
839 Heredity 107: 496–508.

840 Smukowski Heil C. S., Ellison C., Dubin M., Noor M. A. F., 2015 Recombining without
841 Hotspots: A Comprehensive Evolutionary Portrait of Recombination in Two Closely
842 Related Species of Drosophila. Genome Biol. Evol. 7: 2829–42.

843 Stevison L. S., Hoehn K. B., Noor M. A. F., 2011 Effects of Inversions on Within- and Between-
844 Species Recombination and Divergence. Genome Biol. Evol. 3: 830.

845 Stevison L. S., Sefick S., Rushton C., Graze R. M., 2017 Recombination rate plasticity: revealing
846 mechanisms by design. Philos. Trans. R. Soc. Lond. B. Biol. Sci. 372: 20160459.

847 Tang H., Zhang X., Miao C., Zhang J., Ming R., *et al.*, 2015 ALLMAPS: robust scaffold
848 ordering based on multiple maps. Genome Biol. 16: 3.

849 Voorrips R. E., 2002 MapChart: software for the graphical presentation of linkage maps and
850 QTLs. J. Hered. 93: 77–78.

851 Wiley C., Ellison C. K., Shaw K. L., 2012 Widespread genetic linkage of mating signals and
852 preferences in the Hawaiian cricket Laupala. Proc. R. Soc. B Biol. Sci. 279: 1203–1209.

853 Wilfert L., Gadau J., Schmid-Hempel P., 2007 Variation in genomic recombination rates among
854 animal taxa and the case of social insects. Heredity 98: 189–197.

855 Wolf J. B. W., Ellegren H., 2016 Making sense of genomic islands of differentiation in light of
856 speciation. Nat. Rev. Gen. 18: 87–100.

857 Yeaman S., Whitlock M. C., 2011 The genetic architecture of adaptation under migration-
858 selection balance. Evolution 65: 1897–1911.

859 Yeaman S., 2013 Genomic rearrangements and the evolution of clusters of locally adaptive loci.
860 Proc. Natl. Acad. Sci. 110: E1743--E1751.

861

862 **FIGURE LEGENDS**

863 Figure 1. Study design. (A) The phylogenetic relationships of studied *Laupala* species based on a
864 neighbor joining tree generated from genetic distances among the parental lines used in this
865 study. Dashed grey lines connect species pairs that were crossed. (B) Approximate distributions
866 of the studied species on the Big Island of Hawaii. (C) Hypothetical segregation and linkage map
867 construction for five genetic loci A, B, C, D, and E in three crosses of fours species. The genetic
868 distance between the loci is 5 centi-Morgan (cM) in each of the four species. Loci [B,C,D] are
869 inverted in the green and black species. When two species that have alternative karyotypes for
870 the inversion are crossed (pair 2), loci in the inversion will not recombine in the first generation
871 hybrid, resulting in reduced genetic (map) length in the second generation hybrid. Other
872 chromosomal rearrangements will have similar effects. Only if two crosses involve
873 homokaryotypic species pairs that have alternative karyotypes can an inversion be detected in a
874 comparison of intercross linkage maps.
875 Figure 2. Initial linkage maps. Bars represent linkage groups (LG) for ParKoh, KonPar, and
876 PruKoh. Lines within the bars indicate marker positions. The scale on the left measures marker
877 spacing in cM. Blue lines connect markers on the same scaffold between the different maps. The
878 map for ParKoh is shown twice to facilitate comparison across all three maps. See Fig S1 for
879 comprehensive maps.
880 Figure 3. Segregation distortion. For each of the seven autosomal linkage groups within the three
881 comprehensive linkage maps (from top to bottom: ParKoh, KonPar, PruKoh), a sliding window

of the negative log-transformed P-values for the $\chi 2$-square test for deviation from a 1:2:1 segregation ratio is shown across markers with black lines in the top panels. In the panel below, the trace of the frequency of heterozygote genotypes (blue lines) and homozygote genotypes for both parental alleles (black and red lines, respectively) is shown. For each intercross, dashed grey lines indicate P = 0.01 (top panels) or expected allele frequencies based on 1:2:1 inheritance (bottom panels).

Figure 4. Recombination and Marey maps. Gray-scale symbols and lines indicate the relationship between the physical distance (scaffold midposition) in million base pairs on the x-axis and the genetic distance in cM for each of the 8 linkage groups on the left y-axis. Open dots represent the dense ParKoh linkage map, triangles and diamonds that of the KonPar and PruKoh cross, respectively. The corresponding lines (ParKoh: solid, KonPar: dashed, PruKoh: dotted) indicate the fitted smoothing spline (10 degrees of freedom). The red lines (same stroke style) show the first order derivative of the fitted splines and represent the variation in recombination rate (in cM per Mb, on the right y-axis) as a function of physical distance. Grey bars indicate the approximate location of male song rhythm QTL peaks. The yellow star in the LG1 panel highlights the QTL peak that co-localizes with a female preference QTL peak (Shaw & Lesnick 2009).

SUPPLEMENTARY MATERIAL

Table S1. Geographic locations of sampled populations

Table S2. Segregation distortion (count of heterozygotes per genotype) statistics.

Table S3. Summary statistics for anchored assembly

Table S4. Integrated AFLP and SNP map for the *L. kohalensis* x *L. paranigra* cross

905 Figure S1. Comprehensive linkage maps.

906 Figure S2. ALLMAPS output

907 Figure S3. Coverage per cross per linkage group

A

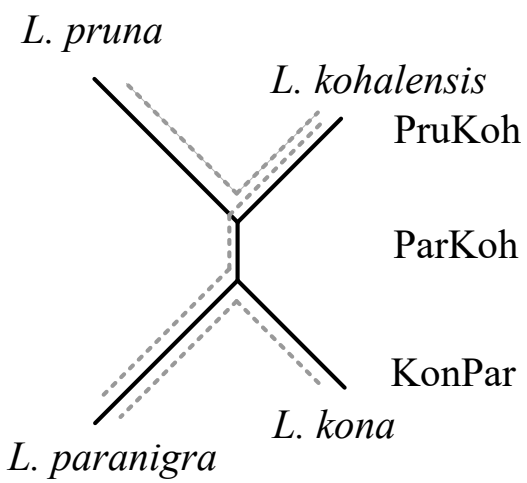

B

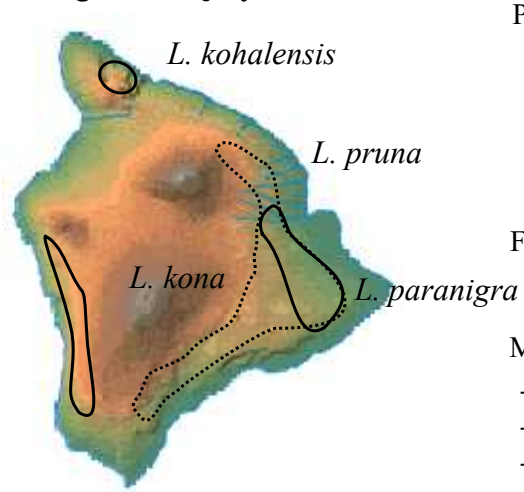

C

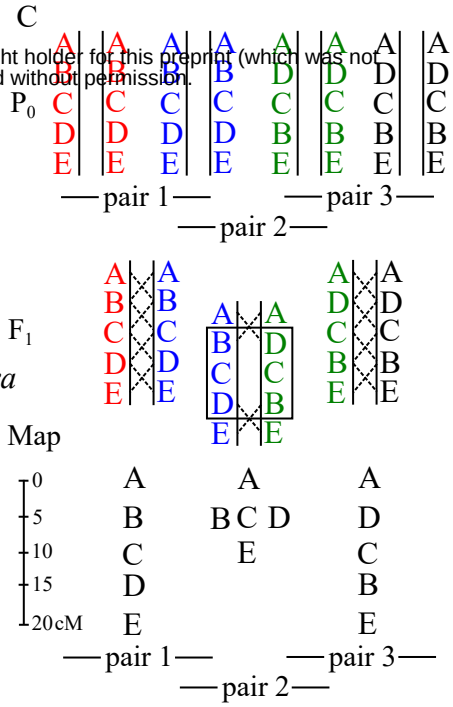

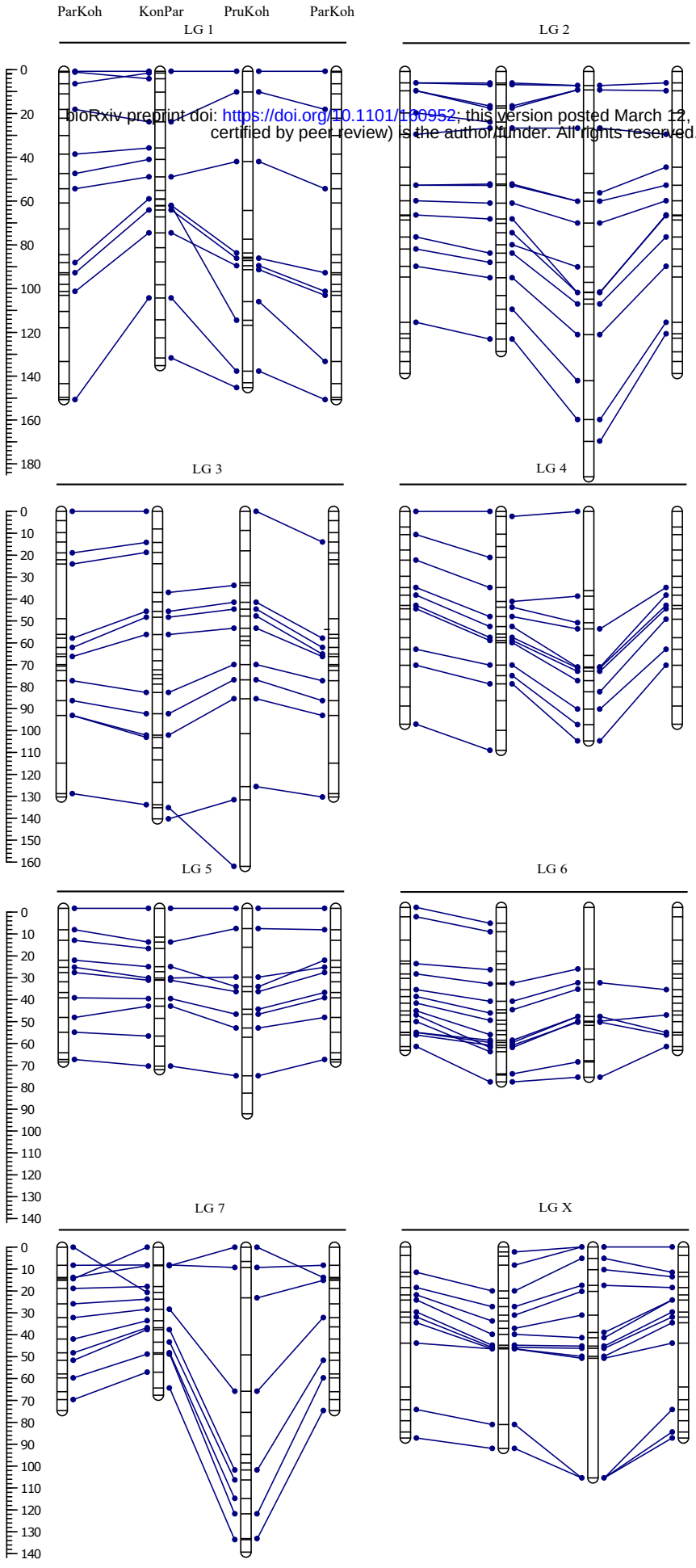

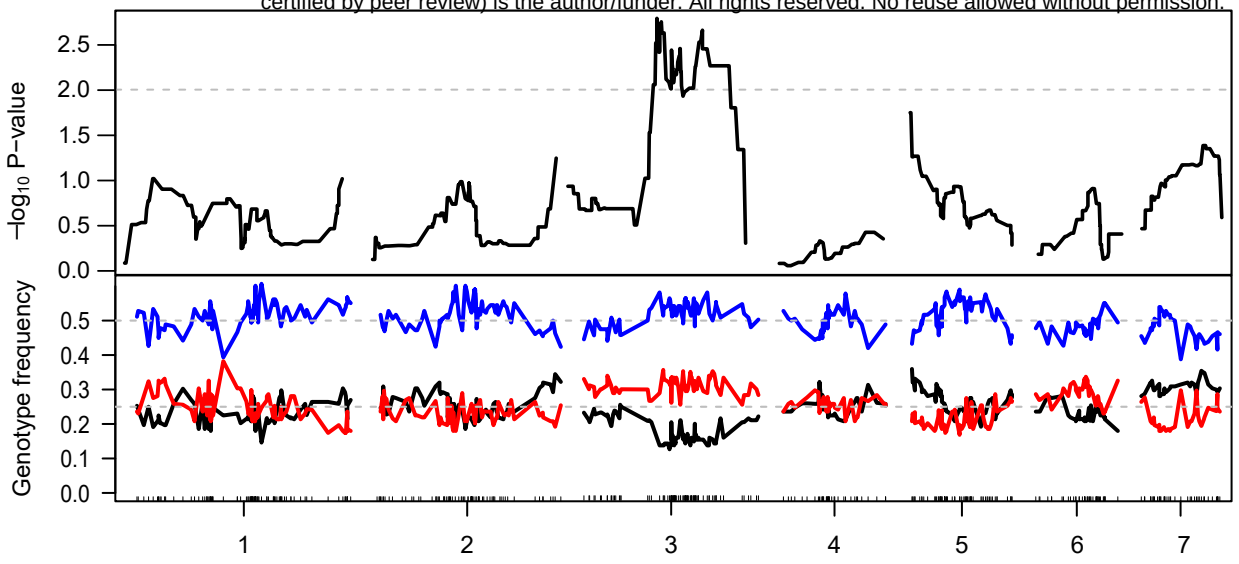

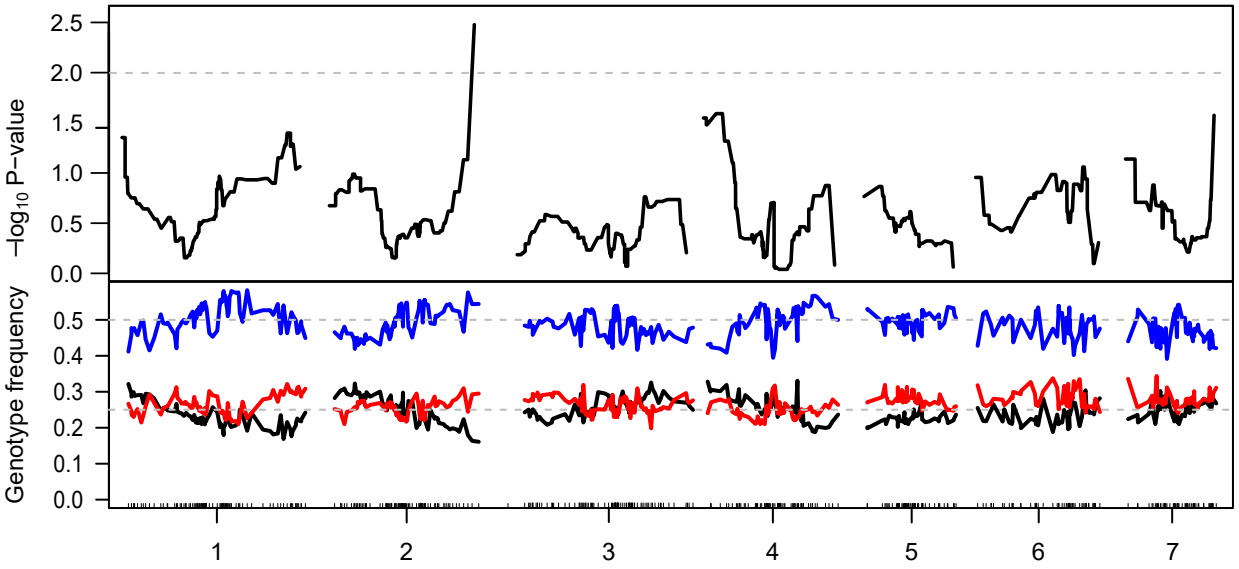

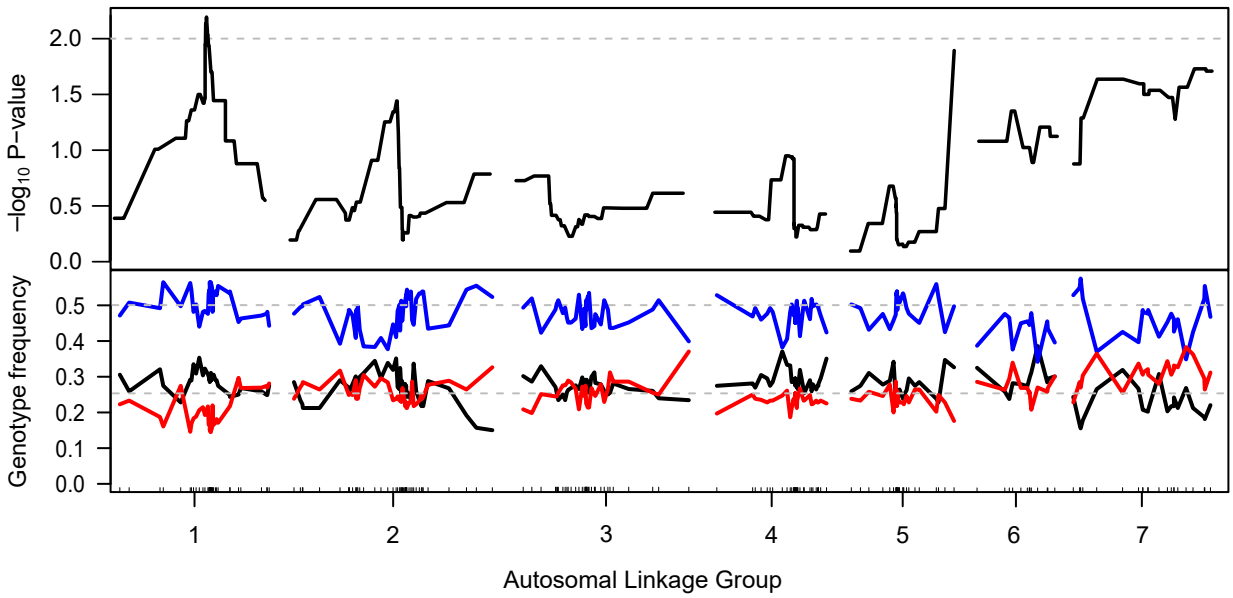

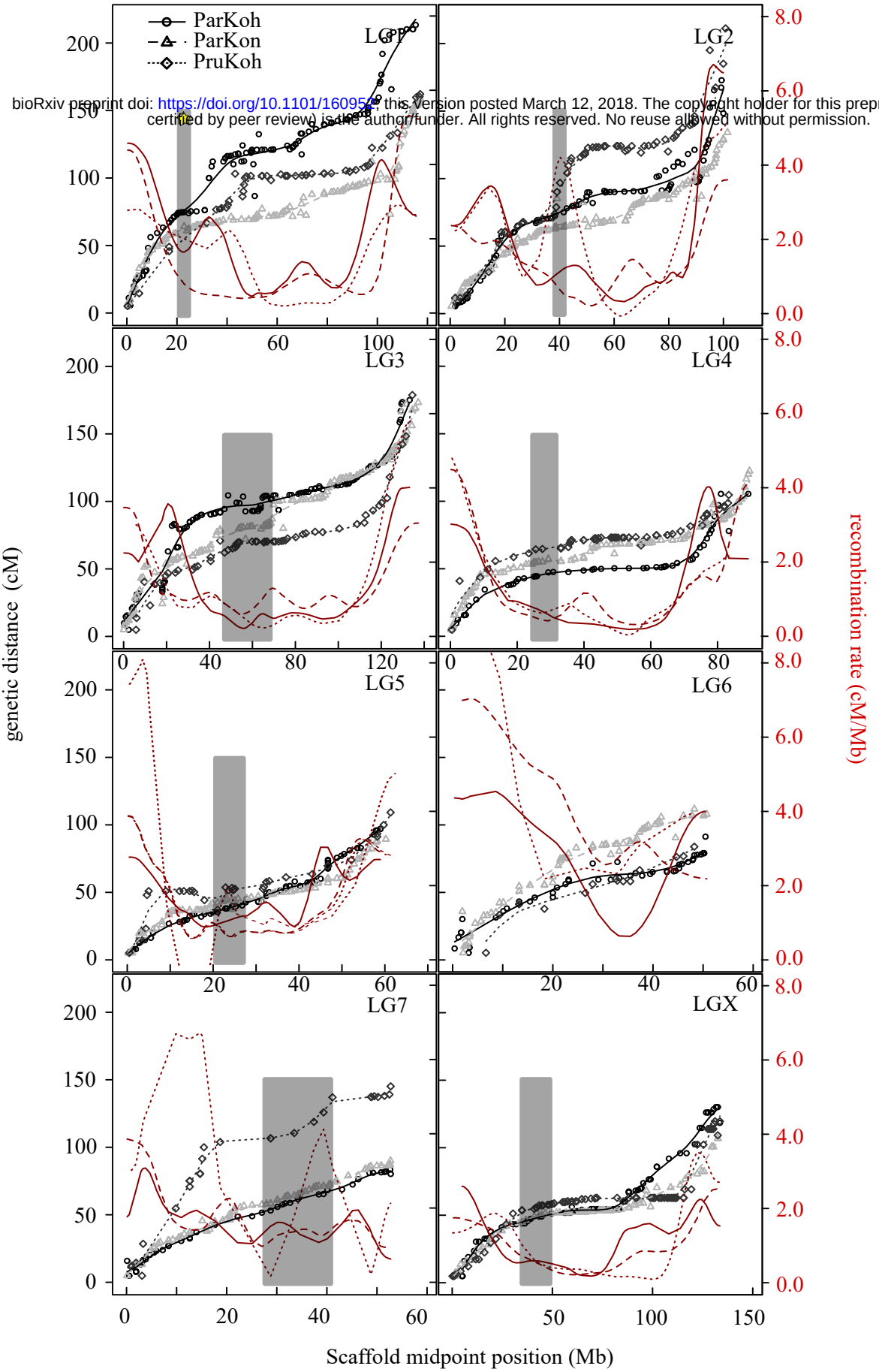

Table S1. Geographic locations of sampled populations

Species	**Locality Name**	**Latitude (N)**	**Longitude (W)**
L. kona	Manuka	19 deg 12'	155 deg 81'
L. paranigra	Kaiwiki	19 deg 46'	155 deg 10'
L. kohalensis	Pololu Valley	20 deg 10'	155 deg 46'
L. pruna	Kaiholena	19 deg 10'	155 deg 35'

Table S2. Segregation distortion (count of heterozygotes per genotype) statistics. *post hoc* Tukey Honest Significant Differences corresponding to the number of heterozygotes (a) across linkage groups (b) across species, (c) and across species nested in linkage groups

contrast	**difference**	**lower bound**	**upper bound**	**P-adjusted**
(a)				
1--3	0.017921	0.009122	0.026719	**0.0000**
2--3	0.008175	-0.00072	0.017069	0.0954
4--3	-0.00601	-0.01562	0.003601	0.5168
5--3	0.008896	-0.00102	0.018812	0.1125
7--3	-0.02664	-0.03742	-0.01586	**0.0000**
6--3	-0.01786	-0.02932	-0.0064	**0.0001**
2--1	-0.00975	-0.01874	-0.00075	**0.0237**
4--1	-0.02393	-0.03364	-0.01423	**0.0000**
5--1	-0.00902	-0.01903	0.000982	0.1086
7--1	-0.04456	-0.05543	-0.0337	**0.0000**
6--1	-0.03578	-0.04732	-0.02425	**0.0000**
4--2	-0.01419	-0.02398	-0.0044	**0.0004**
5--2	0.00072	-0.00937	0.01081	1.0000
7--2	-0.03482	-0.04576	-0.02388	**0.0000**
6--2	-0.02604	-0.03764	-0.01443	**0.0000**
5--4	0.014907	0.004178	0.025637	**0.0009**
7--4	-0.02063	-0.03216	-0.0091	**0.0000**
6--4	-0.01185	-0.02402	0.000318	0.0622
7--5	-0.03554	-0.04732	-0.02375	**0.0000**
6--5	-0.02676	-0.03917	-0.01435	**0.0000**
6--7	0.008781	-0.00433	0.021891	**0.4295**
(b)				
konpar-parkoh	-0.0155	-0.02039	-0.01062	**0.0000**
prukoh-parkoh	-0.02437	-0.03058	-0.01816	**0.0000**
prukoh-konpar	-0.00886	-0.01475	-0.00297	**0.0012**
(c)				

1:parkoh-3:parkoh	-0.00225	-0.01967	1.52E-02	1.0000
2:parkoh-3:parkoh	0.008894	-0.00981	2.76E-02	0.9835
4:parkoh-3:parkoh	-0.02438	-0.0469	-1.87E-03	**0.0178**
5:parkoh-3:parkoh	0.003542	-0.01602	2.31E-02	1.0000
7:parkoh-3:parkoh	-0.05123	-0.07443	-2.80E-02	**0.0000**
6:parkoh-3:parkoh	-0.03392	-0.05676	-1.11E-02	**0.0000**
3:konpar-3:parkoh	-0.03299	-0.04963	-1.63E-02	**0.0000**
1:konpar-3:parkoh	-0.0081	-0.02516	8.96E-03	0.9839
2:konpar-3:parkoh	-0.01921	-0.03615	-2.27E-03	**0.0089**
4:konpar-3:parkoh	-0.01981	-0.03754	-2.07E-03	**0.0113**
5:konpar-3:parkoh	-0.0266	-0.04561	-7.60E-03	**0.0001**
7:konpar-3:parkoh	-0.05016	-0.06964	-3.07E-02	**0.0000**
6:konpar-3:parkoh	-0.03407	-0.05469	-1.35E-02	**0.0000**
3:prukoh-3:parkoh	-0.03762	-0.05901	-1.62E-02	**0.0000**
1:prukoh-3:parkoh	0.000708	-0.02165	2.31E-02	1.0000
2:prukoh-3:parkoh	-0.0359	-0.05673	-1.51E-02	**0.0000**
4:prukoh-3:parkoh	-0.04794	-0.06946	-2.64E-02	**0.0000**
5:prukoh-3:parkoh	-0.01828	-0.04429	7.73E-03	0.5987
7:prukoh-3:parkoh	-0.04113	-0.06927	-1.30E-02	**0.0000**
6:prukoh-3:parkoh	-0.0881	-0.12526	-5.09E-02	**0.0000**
2:parkoh-1:parkoh	0.011142	-0.00727	2.96E-02	0.8411
4:parkoh-1:parkoh	-0.02214	-0.04441	1.39E-04	**0.0537**
5:parkoh-1:parkoh	0.00579	-0.0135	2.51E-02	1.0000
7:parkoh-1:parkoh	-0.04899	-0.07195	-2.60E-02	**0.0000**
6:parkoh-1:parkoh	-0.03167	-0.05428	-9.06E-03	**0.0001**
3:konpar-1:parkoh	-0.03074	-0.04706	-1.44E-02	**0.0000**
1:konpar-1:parkoh	-0.00585	-0.02259	1.09E-02	0.9997
2:konpar-1:parkoh	-0.01696	-0.03359	-3.44E-04	**0.0391**
4:konpar-1:parkoh	-0.01756	-0.03498	-1.32E-04	**0.0457**
5:konpar-1:parkoh	-0.02436	-0.04308	-5.64E-03	**0.0007**
7:konpar-1:parkoh	-0.04791	-0.06712	-2.87E-02	**0.0000**
6:konpar-1:parkoh	-0.03183	-0.05218	-1.15E-02	**0.0000**
3:prukoh-1:parkoh	-0.03537	-0.05651	-1.42E-02	**0.0000**
1:prukoh-1:parkoh	0.002956	-0.01916	2.51E-02	1.0000
2:prukoh-1:parkoh	-0.03366	-0.05422	-1.31E-02	**0.0000**
4:prukoh-1:parkoh	-0.04569	-0.06696	-2.44E-02	**0.0000**
5:prukoh-1:parkoh	-0.01603	-0.04183	9.77E-03	0.8077
7:prukoh-1:parkoh	-0.03888	-0.06683	-1.09E-02	**0.0001**
6:prukoh-1:parkoh	-0.08585	-0.12287	-4.88E-02	**0.0000**
4:parkoh-2:parkoh	-0.03328	-0.05656	-9.99E-03	**0.0001**
5:parkoh-2:parkoh	-0.00535	-0.0258	1.51E-02	1.0000

7:parkoh-2:parkoh	-0.06013	-0.08407	-3.62E-02	**0.0000**
6:parkoh-2:parkoh	-0.04281	-0.06642	-1.92E-02	**0.0000**
3:konpar-2:parkoh	-0.04188	-0.05956	-2.42E-02	**0.0000**
1:konpar-2:parkoh	-0.01699	-0.03506	1.08E-03	**0.0965**
2:konpar-2:parkoh	-0.02811	-0.04606	-1.02E-02	**0.0000**
4:konpar-2:parkoh	-0.0287	-0.0474	-1.00E-02	**0.0000**
5:konpar-2:parkoh	-0.0355	-0.05541	-1.56E-02	**0.0000**
7:konpar-2:parkoh	-0.05905	-0.07942	-3.87E-02	**0.0000**
6:konpar-2:parkoh	-0.04297	-0.06442	-2.15E-02	**0.0000**
3:prukoh-2:parkoh	-0.04651	-0.06872	-2.43E-02	**0.0000**
1:prukoh-2:parkoh	-0.00819	-0.03132	1.49E-02	0.9997
2:prukoh-2:parkoh	-0.0448	-0.06645	-2.31E-02	**0.0000**
4:prukoh-2:parkoh	-0.05684	-0.07916	-3.45E-02	**0.0000**
5:prukoh-2:parkoh	-0.02717	-0.05385	-4.95E-04	**0.0402**
7:prukoh-2:parkoh	-0.05003	-0.07879	-2.13E-02	**0.0000**
6:prukoh-2:parkoh	-0.09699	-0.13463	-5.94E-02	**0.0000**
5:parkoh-4:parkoh	0.027926	0.003943	5.19E-02	**0.0058**
7:parkoh-4:parkoh	-0.02685	-0.05388	1.77E-04	**0.0539**
6:parkoh-4:parkoh	-0.00953	-0.03626	1.72E-02	0.9996
3:konpar-4:parkoh	-0.0086	-0.03027	1.31E-02	0.9982
1:konpar-4:parkoh	0.016287	-0.0057	3.83E-02	0.4920
2:konpar-4:parkoh	0.005171	-0.01673	2.71E-02	1.0000
4:konpar-4:parkoh	0.004578	-0.01794	2.71E-02	1.0000
5:konpar-4:parkoh	-0.00222	-0.02575	2.13E-02	1.0000
7:konpar-4:parkoh	-0.02577	-0.04969	-1.85E-03	**0.0192**
6:konpar-4:parkoh	-0.00969	-0.03454	1.52E-02	0.9986
3:prukoh-4:parkoh	-0.01323	-0.03873	1.23E-02	0.9584
1:prukoh-4:parkoh	0.025092	-0.00122	5.14E-02	**0.0841**
2:prukoh-4:parkoh	-0.01152	-0.03654	1.35E-02	0.9886
4:prukoh-4:parkoh	-0.02356	-0.04916	2.05E-03	**0.1190**
5:prukoh-4:parkoh	0.006104	-0.02337	3.56E-02	1.0000
7:prukoh-4:parkoh	-0.01675	-0.04812	1.46E-02	0.9452
6:prukoh-4:parkoh	-0.06372	-0.10339	-2.40E-02	**0.0000**
7:parkoh-5:parkoh	-0.05478	-0.0794	-3.02E-02	**0.0000**
6:parkoh-5:parkoh	-0.03746	-0.06175	-1.32E-02	**0.0000**
3:konpar-5:parkoh	-0.03653	-0.05511	-1.79E-02	**0.0000**
1:konpar-5:parkoh	-0.01164	-0.03059	7.32E-03	0.8233
2:konpar-5:parkoh	-0.02275	-0.0416	-3.91E-03	**0.0031**
4:konpar-5:parkoh	-0.02335	-0.04291	-3.79E-03	**0.0038**
5:konpar-5:parkoh	-0.03015	-0.05087	-9.42E-03	**0.0000**
7:konpar-5:parkoh	-0.0537	-0.07486	-3.25E-02	**0.0000**

6:konpar-5:parkoh	-0.03761	-0.05982	-1.54E-02	**0.0000**
3:prukoh-5:parkoh	-0.04116	-0.0641	-1.82E-02	**0.0000**
1:prukoh-5:parkoh	-0.00283	-0.02667	2.10E-02	1.0000
2:prukoh-5:parkoh	-0.03944	-0.06185	-1.70E-02	**0.0000**
4:prukoh-5:parkoh	-0.05148	-0.07454	-2.84E-02	**0.0000**
5:prukoh-5:parkoh	-0.02182	-0.04911	5.47E-03	0.3364
7:prukoh-5:parkoh	-0.04467	-0.074	-1.53E-02	**0.0000**
6:prukoh-5:parkoh	-0.09164	-0.12971	-5.36E-02	**0.0000**
6:parkoh-7:parkoh	0.017315	-0.00999	4.46E-02	0.7787
3:konpar-7:parkoh	0.018246	-0.00413	4.06E-02	0.2992
1:konpar-7:parkoh	0.043137	0.020451	6.58E-02	**0.0000**
2:konpar-7:parkoh	0.032021	0.009425	5.46E-02	**0.0001**
4:konpar-7:parkoh	0.031428	0.008233	5.46E-02	**0.0003**
5:konpar-7:parkoh	0.02463	0.000448	4.88E-02	**0.0402**
7:konpar-7:parkoh	0.001077	-0.02349	2.56E-02	1.0000
6:konpar-7:parkoh	0.017161	-0.00831	4.26E-02	0.6787
3:prukoh-7:parkoh	0.013617	-0.01249	3.97E-02	0.9562
1:prukoh-7:parkoh	0.051942	0.025044	7.88E-02	**0.0000**
2:prukoh-7:parkoh	0.015331	-0.0103	4.10E-02	0.8547
4:prukoh-7:parkoh	0.003292	-0.02291	2.95E-02	1.0000
5:prukoh-7:parkoh	0.032954	0.002954	6.30E-02	**0.0145**
7:prukoh-7:parkoh	0.010102	-0.02176	4.20E-02	0.9999
6:prukoh-7:parkoh	-0.03687	-0.07693	3.19E-03	0.1187
3:konpar-6:parkoh	0.000931	-0.02108	2.29E-02	1.0000
1:konpar-6:parkoh	0.025822	0.003496	4.81E-02	**0.0065**
2:konpar-6:parkoh	0.014706	-0.00753	3.69E-02	0.7117
4:konpar-6:parkoh	0.014113	-0.00873	3.70E-02	0.8152
5:konpar-6:parkoh	0.007315	-0.01653	3.12E-02	1.0000
7:konpar-6:parkoh	-0.01624	-0.04047	7.99E-03	0.6886
6:konpar-6:parkoh	-0.00015	-0.0253	2.50E-02	1.0000
3:prukoh-6:parkoh	-0.0037	-0.02949	2.21E-02	1.0000
1:prukoh-6:parkoh	0.034627	0.008032	6.12E-02	**0.0007**
2:prukoh-6:parkoh	-0.00198	-0.0273	2.33E-02	1.0000
4:prukoh-6:parkoh	-0.01402	-0.03992	1.19E-02	0.9374
5:prukoh-6:parkoh	0.015639	-0.01409	4.54E-02	0.9525
7:prukoh-6:parkoh	-0.00721	-0.03882	2.44E-02	1.0000
6:prukoh-6:parkoh	-0.05418	-0.09404	-1.43E-02	**0.0003**
1:konpar-3:konpar	0.024891	0.008963	4.08E-02	**0.0000**
2:konpar-3:konpar	0.013775	-0.00202	2.96E-02	0.1878
4:konpar-3:konpar	0.013182	-0.00346	2.98E-02	0.3552
5:konpar-3:konpar	0.006384	-0.01161	2.44E-02	0.9996

7:konpar-3:konpar	-0.01717	-0.03567	1.33E-03	**0.1099**
6:konpar-3:konpar	-0.00109	-0.02077	1.86E-02	1.0000
3:prukoh-3:konpar	-0.00463	-0.02513	1.59E-02	1.0000
1:prukoh-3:konpar	0.033696	0.012189	5.52E-02	**0.0000**
2:prukoh-3:konpar	-0.00291	-0.02282	1.70E-02	1.0000
4:prukoh-3:konpar	-0.01495	-0.03559	5.68E-03	0.5369
5:prukoh-3:konpar	0.014708	-0.01057	4.00E-02	0.8830
7:prukoh-3:konpar	-0.00814	-0.03561	1.93E-02	1.0000
6:prukoh-3:konpar	-0.05511	-0.09177	-1.85E-02	**0.0000**
2:konpar-1:konpar	-0.01112	-0.02735	5.12E-03	0.6496
4:konpar-1:konpar	-0.01171	-0.02877	5.35E-03	0.6448
5:konpar-1:konpar	-0.01851	-0.03689	-1.26E-04	**0.0461**
7:konpar-1:konpar	-0.04206	-0.06094	-2.32E-02	**0.0000**
6:konpar-1:konpar	-0.02598	-0.04602	-5.94E-03	**0.0007**
3:prukoh-1:konpar	-0.02952	-0.05036	-8.68E-03	**0.0001**
1:prukoh-1:konpar	0.008805	-0.01303	3.06E-02	0.9978
2:prukoh-1:konpar	-0.02781	-0.04806	-7.55E-03	**0.0002**
4:prukoh-1:konpar	-0.03984	-0.06082	-1.89E-02	**0.0000**
5:prukoh-1:konpar	-0.01018	-0.03574	1.54E-02	0.9982
7:prukoh-1:konpar	-0.03304	-0.06076	-5.31E-03	**0.0039**
6:prukoh-1:konpar	-0.08	-0.11685	-4.32E-02	**0.0000**
4:konpar-2:konpar	-0.00059	-0.01753	1.63E-02	1.0000
5:konpar-2:konpar	-0.00739	-0.02566	1.09E-02	0.9977
7:konpar-2:konpar	-0.03094	-0.04972	-1.22E-02	**0.0000**
6:konpar-2:konpar	-0.01486	-0.0348	5.08E-03	0.4790
3:prukoh-2:konpar	-0.0184	-0.03915	2.34E-03	0.1635
1:prukoh-2:konpar	0.019921	-0.00182	4.17E-02	0.1233
2:prukoh-2:konpar	-0.01669	-0.03684	3.46E-03	0.2713
4:prukoh-2:konpar	-0.02873	-0.0496	-7.85E-03	**0.0002**
5:prukoh-2:konpar	0.000933	-0.02454	2.64E-02	1.0000
7:prukoh-2:konpar	-0.02192	-0.04957	5.73E-03	0.3532
6:prukoh-2:konpar	-0.06889	-0.10568	-3.21E-02	**0.0000**
5:konpar-4:konpar	-0.0068	-0.0258	1.22E-02	0.9996
7:konpar-4:konpar	-0.03035	-0.04984	-1.09E-02	**0.0000**
6:konpar-4:konpar	-0.01427	-0.03488	6.35E-03	0.6288
3:prukoh-4:konpar	-0.01781	-0.03921	3.59E-03	0.2622
1:prukoh-4:konpar	0.020514	-0.00184	4.29E-02	0.1220
2:prukoh-4:konpar	-0.0161	-0.03692	4.73E-03	0.4037
4:prukoh-4:konpar	-0.02814	-0.04966	-6.61E-03	**0.0006**
5:prukoh-4:konpar	0.001526	-0.02448	2.75E-02	1.0000
7:prukoh-4:konpar	-0.02133	-0.04947	6.81E-03	0.4444

6:prukoh-4:konpar	-0.06829	-0.10546	-3.11E-02	**0.0000**
7:konpar-5:konpar	-0.02355	-0.04421	-2.90E-03	**0.0081**
6:konpar-5:konpar	-0.00747	-0.02919	1.43E-02	0.9998
3:prukoh-5:konpar	-0.01101	-0.03348	1.15E-02	0.9769
1:prukoh-5:konpar	0.027312	0.00393	5.07E-02	**0.0055**
2:prukoh-5:konpar	-0.0093	-0.03122	1.26E-02	0.9958
4:prukoh-5:konpar	-0.02134	-0.04392	1.24E-03	**0.0922**
5:prukoh-5:konpar	0.008324	-0.01857	3.52E-02	1.0000
7:prukoh-5:konpar	-0.01453	-0.04349	1.44E-02	0.9705
6:prukoh-5:konpar	-0.0615	-0.09928	-2.37E-02	**0.0000**
6:konpar-7:konpar	0.016084	-0.00606	3.82E-02	0.5321
3:prukoh-7:konpar	0.01254	-0.01033	3.54E-02	0.9299
1:prukoh-7:konpar	0.050865	0.02709	7.46E-02	**0.0000**
2:prukoh-7:konpar	0.014254	-0.00808	3.66E-02	0.7695
4:prukoh-7:konpar	0.002215	-0.02077	2.52E-02	1.0000
5:prukoh-7:konpar	0.031877	0.004642	5.91E-02	**0.0053**
7:prukoh-7:konpar	0.009024	-0.02025	3.83E-02	1.0000
6:prukoh-7:konpar	-0.03794	-0.07598	8.89E-05	0.0514
3:prukoh-6:konpar	-0.00354	-0.02738	2.03E-02	1.0000
1:prukoh-6:konpar	0.034781	0.010074	5.95E-02	**0.0001**
2:prukoh-6:konpar	-0.00183	-0.02516	2.15E-02	1.0000
4:prukoh-6:konpar	-0.01387	-0.03782	1.01E-02	0.8876
5:prukoh-6:konpar	0.015793	-0.01226	4.38E-02	0.9112
7:prukoh-6:konpar	-0.00706	-0.0371	2.30E-02	1.0000
6:prukoh-6:konpar	-0.05403	-0.09265	-1.54E-02	**0.0001**
1:prukoh-3:prukoh	0.038325	0.012961	6.37E-02	**0.0000**
2:prukoh-3:prukoh	0.001714	-0.02231	2.57E-02	1.0000
4:prukoh-3:prukoh	-0.01032	-0.03495	1.43E-02	0.9964
5:prukoh-3:prukoh	0.019338	-0.0093	4.80E-02	0.6747
7:prukoh-3:prukoh	-0.00352	-0.0341	2.71E-02	1.0000
6:prukoh-3:prukoh	-0.05048	-0.08953	-1.14E-02	**0.0008**
2:prukoh-1:prukoh	-0.03661	-0.06149	-1.17E-02	**0.0000**
4:prukoh-1:prukoh	-0.04865	-0.07412	-2.32E-02	**0.0000**
5:prukoh-1:prukoh	-0.01899	-0.04835	1.04E-02	0.7487
7:prukoh-1:prukoh	-0.04184	-0.0731	-1.06E-02	**0.0004**
6:prukoh-1:prukoh	-0.08881	-0.12839	-4.92E-02	**0.0000**
4:prukoh-2:prukoh	-0.01204	-0.03617	1.21E-02	0.9722
5:prukoh-2:prukoh	0.017623	-0.01058	4.58E-02	0.8001
7:prukoh-2:prukoh	-0.00523	-0.03541	2.50E-02	1.0000
6:prukoh-2:prukoh	-0.0522	-0.09093	-1.35E-02	**0.0003**
5:prukoh-4:prukoh	0.029662	0.000935	5.84E-02	**0.0339**

7:prukoh-4:prukoh	0.006809	-0.02386	3.75E-02	1.0000
6:prukoh-4:prukoh	-0.04016	-0.07927	-1.04E-03	**0.0364**
7:prukoh-5:prukoh	-0.02285	-0.05682	1.11E-02	0.6817
6:prukoh-5:prukoh	-0.06982	-0.11157	-2.81E-02	**0.0000**
6:prukoh-7:prukoh	-0.04697	-0.09008	-3.86E-03	**0.0164**

Table S3. Summary statistics for anchored assembly. For each cross and for the combined pseudomolecule assembly the number of scaffolds with at least 2 markers, with at least two markers that are > 0.1 cM apart, the combined size of the anchored scaffolds, the N50, and the average coverage are shown per LG.

LG	**# scaffolds**	**# scaffolds >= 2 markers**	**# scaffolds >=2 well-spaced markers**	**Size (bp)**	**N50 (bp)**	**coverage**
ParKoh						
1	117	21	14	106312036	1301586	52.89792
2	89	8	4	59124686	886001	54.757
3	109	14	12	98715872	1184645	51.15361
4	49	1	1	39589978	1093907	54.17022
5	76	18	16	62735740	1197186	66.5671
6	47	7	6	19057194	730017	57.78891
7	45	6	5	38543039	1485176	60.40972
X	76	4	2	84017840	1519936	29.56227
Sum/median	608	79	60	508096385	1190916	53.41334375
KonPar						
1	128	17	13	103734776	1143465	37.22859
2	132	17	10	95158272	1019600	40.18552
3	143	22	19	134318749	1355019	34.98008
4	109	24	12	110192983	1660236	40.38131
5	84	13	9	67417874	1136159	44.86084
6	64	7	6	23922075	733389	46.43391
7	77	17	13	58701654	1180700	38.07606
X	86	14	3	98541466	1540389	25.64274
Sum/median	823	131	85	691987849	1162083	38.47363125
PruKoh						
1	50	5	3	46785714	1325001	41.55226
2	62	4	3	45819772	1106261	47.8152
3	57	2	2	54629290	1375220	40.13577
4	56	11	5	60827800	2025849	45.12183
5	33	3	2	20743600	725518	51.94363
6	14	0	0	7779385	859092	45.60227
7	27	4	2	17783624	1224531	49.36982
X	84	9	0	82253003	1268875	28.72471

Sum/median	383	38	17	336622188	1246703	43.78318625
Combined						
1	167	43	30	117180395	1089296	
2	170	29	17	101876544	816734	
3	175	38	33	137279277	1044733	
4	118	36	18	89703238	957048	
5	102	34	27	62192538	880080	
6	80	14	12	25387579	569059	
7	88	27	20	52742540	916807	
X	154	27	5	133989488	1249941	
Sum/median	1054	248	162	720351599	936928	

Table S4. Integrated AFLP and SNP map for the *L. kohalensis* x *L. paranigra* cross. The highlighted AFLP markers are located under a QTL peak in the Shaw & Lesnick 2009 study. The highlighted AFLP markers on linkage group 1 are markers where a male song and female preference QTL peak co-localize.

scaffold	locus	LG	position (cM)	AFLP	scaffold midpoint position (bp)
S002761	S002761_729410	1	0	NA	106423286
	as030	1	1.821	PaggcA53	NA
	as074	1	3.282	PggacA54	NA
	ac007	1	6.09	PagacA52B55	NA
	ac013	1	7.301	PcgacA51B51	NA
	ac017	1	8.604	PgcacA07B54	NA
S000817	S000817_120415	1	9.734	NA	114208815
S002077	S002077_311803	1	11.288	NA	109788919
S007909	S007909_155126	1	13.752	NA	104812030
	as087	1	23.642	PgtgcA54	NA
	as081	1	25.658	PgtacA56	NA
	as085_x	1	30.736	PgtgcA3	NA
	as080	1	36.928	PgtacA55	NA
	as023	1	38.868	PaaacA63	NA
S001330	S001330_135948	1	42.507	NA	100949675
S001771	S001771_116507	1	46.906	NA	105601414
S000392	S000392_74030	1	51.737	NA	NA
S001680	S001680_315523	1	52.615	NA	88172650
S000409	S000409_474112	1	53.517	NA	84174036
S001489	S001489_769426	1	56.166	NA	41585373
S004205	S004205_29098	1	57.827	NA	50498860

S000949	S000949_205067	1	58.259	NA	42520204
S008139	S008139_68543	1	58.542	NA	NA
S000696	S000696_137337	1	58.549	NA	NA
S002946	S002946_738803	1	58.707	NA	67349798
C120306	C120306_385	1	58.847	NA	NA
S006572	S006572_95801	1	58.928	NA	46181571
S001914	S001914_404347	1	59.118	NA	66160290
S009296	S009296_110864	1	59.329	NA	65039174
S000663	S000663_611964	1	59.641	NA	53947499
S004747	S004747_292840	1	59.784	NA	49933664
S000671	S000671_1033505	1	61.079	NA	NA
S001489	S001489_639186	1	61.694	NA	41585373
S004313	S004313_69835	1	61.699	NA	40812282
S002548	S002548_423714	1	62.493	NA	45749393
S000105	S000105_348801	1	63.591	NA	36945493
S004771	S004771_628132	1	64.917	NA	31081394
S004771	S004771_1175996	1	65.21	NA	31081394
S002151	S002151_1377807	1	66.292	NA	22870317
	as034	1	68.191	PatgcA52	NA
	as012	1	70.107	PccacA55	NA
	ac014	2	0	PgaacA10B60	NA
S001206	S001206_1546586	2	2.303	NA	1821533
S000518	S000518_766492	2	6.245	NA	6192438
	as077	2	26.628	PgggcA52	NA
S003191	S003191_528616	2	31.612	NA	16874625
S001838	S001838_6021	2	42.989	NA	23233385
S000416	S000416_552586	2	47.133	NA	24694735
S004218	S004218_23553	2	51.627	NA	31927917
S001550	S001550_214202	2	52.41	NA	33996652
S003798	S003798_463488	2	53.5	NA	36725738
S002376	S002376_431585	2	54.951	NA	38303813
	as052	2	57.787	PcggcA53	NA
S005289	S005289_526503	2	58.474	NA	45049140
S000230	S000230_200879	2	58.756	NA	46073354
S002156	S002156_413885	2	61.643	NA	90147661
S003079	S003079_192141	2	61.705	NA	56392065
S004728	S004728_52289	2	61.99	NA	77439224
S001050	S001050_43796	2	62.025	NA	71210412
S001881	S001881_642832	2	62.193	NA	60129008
S003118	S003118_235274	2	62.379	NA	56724422
S003735	S003735_82587	2	62.896	NA	NA

	ac006	2	63.793	PacacA56B69	NA
	as040_x	2	64.823	PcagcA08	NA
S003067	S003067_20757	2	67.28	NA	80842581
S000199	S000199_193260	2	74.457	NA	83353553
S001797	S001797_1827615	2	75.671	NA	85052994
S001855	S001855_342231	2	82.018	NA	89412353
S004792	S004792_152639	2	85.245	NA	NA
S001901	S001901_315332	2	87.985	NA	94264609
S001602	S001602_266912	2	109.791	NA	99970919
S000793	S000793_627068	2	116.258	NA	NA
	as115	3	0	PttacA54	NA
	as083	3	3.848	PgtacA58	NA
S001338	S001338_29965	3	5.698	NA	168668
	as037	3	9.753	PcaacA57	NA
S000075	S000075_156551	3	11.248	NA	1642392
S002528	S002528_794391	3	19.911	NA	18001031
S009989	S009989_70944	3	21.779	NA	6045815
S002528	S002528_794393	3	23.255	NA	18001031
S005403	S005403_7134	3	27.914	NA	18662141
	ac009_a	3	48.316	PaggcA07B19	NA
	as063	3	49.481	PgaacA60	NA
	as064	3	51.877	PgaacA61	NA
	as025	3	53.754	PaagcA57	NA
S000558	S000558_1959639	3	59.995	NA	40534699
S000558	S000558_1232157	3	60.337	NA	40534699
	as088	3	63.867	PgtgcA55	NA
	as069	3	64.465	PgcacA51	NA
	ad100.as079	3	65.149	NA	NA
S004777	S004777_221108	3	66.442	NA	36430961
S000558	S000558_748836	3	66.865	NA	40534699
S007419	S007419_788393	3	67.162	NA	42061284
S002934	S002934_242739	3	68.016	NA	56760880
S003072	S003072_393178	3	68.244	NA	63064570
S001785	S001785_133632	3	68.301	NA	60906412
S000726	S000726_1782089	3	68.399	NA	48678466
S000529	S000529_530363	3	68.572	NA	72186930
	as108_a	3	68.59	PtgacA03	NA
S002665	S002665_282741	3	68.951	NA	NA
S005483	S005483_46807	3	69.079	NA	62650842
S013086	S013086_40139	3	69.12	NA	NA
S002194	S002194_96231	3	69.157	NA	66669112

S006750	S006750_274965	3	69.245	NA	NA
S004654	S004654_237626	3	69.303	NA	NA
S002002	S002002_376411	3	69.412	NA	44975632
S003472	S003472_9538	3	70.555	NA	82404642
S002613	S002613_31096	3	71.526	NA	NA
S001060	S001060_728231	3	72.259	NA	89191537
S002297	S002297_775779	3	72.322	NA	91133138
S001060	S001060_1929755	3	72.461	NA	89191537
S006865	S006865_338439	3	72.867	NA	101275163
	as101	3	73.62	PtcgcA09	NA
S001265	S001265_211884	3	74.555	NA	106649134
S000385	S000385_1480834	3	75.848	NA	108764126
S001106	S001106_481878	3	82.071	NA	114989880
	as114_ax	3	86.713	PttacA02	NA
S001275	S001275_1127865	3	88.98	NA	122746700
S002311	S002311_254807	3	89.321	NA	123571440
	as076_a	4	0	PgggcA01	NA
	as073_a	4	1.753	PggacA01	NA
S005844	S005844_224400	4	18.591	NA	4097279
	as117_a	4	41.053	PttacA06	NA
	as099	4	41.551	PtcacA54	NA
S001783	S001783_279356	4	43.04	NA	63112104
S000590	S000590_1997032	4	43.249	NA	29331168
S014891	S014891_36875	4	43.589	NA	NA
S003206	S003206_599818	4	43.711	NA	NA
S000836	S000836_228275	4	43.801	NA	NA
S000679	S000679_623688	4	43.895	NA	57825201
	as075_a	4	44.445	PggacA13	NA
S002196	S002196_584574	4	44.674	NA	42514727
S001005	S001005_1065597	4	44.857	NA	39878575
S003635	S003635_7993	4	45.443	NA	63978342
S009873	S009873_154713	4	49.074	NA	71866807
S002058	S002058_706797	4	49.408	NA	72523035
S000455	S000455_692625	4	52.283	NA	73544308
	as029_a	4	61.5	PagacA5	NA
S001486	S001486_61579	4	64.17	NA	77623428
	as028_x	4	65.829	PagacA1	NA
S001279	S001279_277406	4	67.269	NA	78135382
S001608	S001608_399358	4	83.462	NA	89198891
	as021	5	0	PaaacA54	NA
S005326	S005326_57790	5	1.807	NA	466530

	ac016	5	2.394	PgagcA56B62	NA
	ac011	5	4.24	PcagcA52B53	NA
	ac015	5	5.865	PgaacA62B66	NA
	as116_a	5	7.016	PttacA05	NA
S002190	S002190_273188	5	13.671	NA	3452268
	as100	5	15.717	PtcgcA54	NA
S000809	S000809_365747	5	19.221	NA	6005121
	as066_a	5	21.423	PgagcA08	NA
	as027_a	5	25.245	PacacA06	NA
	ad082.as062	5	26.337	NA	NA
	as045	5	27.055	PccacA53	NA
S004462	S004462_54127	5	28.207	NA	13078451
S005610	S005610_84211	5	28.338	NA	13179099
S000366	S000366_42046	5	28.803	NA	17964325
S000745	S000745_339612	5	30.425	NA	21039003
S002565	S002565_116928	5	33.166	NA	22902902
S004683	S004683_48328	5	34.768	NA	24389284
S006506	S006506_7146	5	35.301	NA	27839633
S005519	S005519_111372	5	37.975	NA	32385211
S000305	S000305_70577	5	40.26	NA	33073185
S000979	S000979_164421	5	41.485	NA	35633669
S005459	S005459_70152	5	42.698	NA	37847956
S000180	S000180_656202	5	44.503	NA	40272446
S021890	S021890_296	5	45.368	NA	42534517
	as068	5	46.655	PgagcA51	NA
S005334	S005334_732385	5	48.033	NA	43080568
S005064	S005064_175253	5	49.954	NA	45035858
	as091	5	52.052	PtaacA51	NA
S003838	S003838_738497	5	54.849	NA	46738481
S001560	S001560_398299	5	59.376	NA	50508185
S004681	S004681_23198	5	61.431	NA	53592894
	as057	5	62.937	PctacA55	NA
	as058	5	63.812	PctacA56	NA
	as059	5	65.211	PctacA57	NA
	as043	5	71.183	PcagcA51	NA
	as118_x	5	72.676	PttacA13	NA
	as041	5	73.969	PcagcA56	NA
S007270	S007270_308120	5	76.332	NA	58235091
S002503	S002503_741242	5	77.495	NA	58956874
	as110	6	0	PtggcA52	NA
	as047_x	6	1.51	PcgacA02	NA

S001034	S001034_78522	6	2.72	NA	24400658
S022584	S022584_1139	6	5.895	NA	23964288
	as105	6	6.664	PtgacA58	NA
S005236	S005236_14409	6	7.404	NA	16442306
S001507	S001507_262717	6	8.078	NA	13978219
S002799	S002799_37080	6	10.159	NA	22063251
	ac003	6	11.251	PaagcA61B63	NA
	ac019	6	13.745	PtgacA57B60	NA
S001904	S001904_134885	6	15.337	NA	16620760
	as109	6	17.735	PtgacA56	NA
	as039	6	20.554	PcagcA54	NA
S000218	S000218_4280	6	21.865	NA	10002544
S001761	S001761_1745572	6	27.303	NA	6635712
S005439	S005439_103276	6	35.966	NA	4315651
S011721	S011721_76537	6	47.364	NA	849742
S003103	S003103_949190	7	0	NA	1904957
S008107	S008107_29859	7	3.613	NA	2842152
S003103	S003103_1019194	7	3.994	NA	1904957
S000557	S000557_589404	7	7.085	NA	3829489
S002304	S002304_728504	7	9.873	NA	4666925
S002736	S002736_346176	7	10.997	NA	5494164
S002736	S002736_115345	7	12.279	NA	5494164
S014172	S014172_53634	7	13.346	NA	5971292
S000628	S000628_1159720	7	17.535	NA	8386281
S000628	S000628_169050	7	18.732	NA	8386281
	as033	7	21.278	PatacA55	NA
	as071_a	7	22.74	PgcgcA11	NA
S000677	S000677_527760	7	24.152	NA	12625625
	as070_a	7	26.358	PgcacA10	NA
S002087	S002087_530732	7	44.525	NA	31673319
S004909	S004909_906373	7	50.728	NA	39335421
S010292	S010292_145463	7	53.418	NA	40115847
S004220	S004220_129736	7	53.983	NA	43031005
S001469	S001469_584893	7	65.118	NA	50836753
S002493	S002493_175861	7	67.129	NA	48491131
	xs032_x	X	0	PttacA04	NA
S000571	S000571_30159	X	2.403	NA	4915702
	xd024	X	11.115	PtagcB55	NA
S001780	S001780_509180	X	24.446	NA	10902308
	xd004	X	25.132	PatacB52	NA
	xs020	X	29.168	PatgcA56	NA

S000766	S000766_827724	X	30.52	NA	11869181
S000360	S000360_70566	X	32.459	NA	17072014
S003455	S003455_1122569	X	35.526	NA	19186595
S004887	S004887_81621	X	42.013	NA	NA
	xs024_x	X	43.011	PcggcA10	NA
S000604	S000604_43741	X	43.459	NA	NA
S000648	S000648_2315784	X	44.883	NA	34819414
S000219	S000219_2024096	X	45.729	NA	26925418
S000777	S000777_1339236	X	46.733	NA	30344332
S000777	S000777_461461	X	46.887	NA	30344332
S000648	S000648_2255296	X	47.453	NA	34819414
S001873	S001873_641123	X	49.384	NA	36757980
	xd016_x	X	49.672	PatgcB02	NA
S001241	S001241_171252	X	53.266	NA	44632865
S003053	S003053_264327	X	55.937	NA	56937852
S000327	S000327_278424	X	56.293	NA	55828014
S000470	S000470_76715	X	56.911	NA	59714238
	xd008_x	X	57.404	PgggcB22	NA
S003307	S003307_279141	X	57.747	NA	63486064
S001912	S001912_587919	X	58.069	NA	62108629
S000965	S000965_1228070	X	59.663	NA	73444967
S000808	S000808_1583160	X	59.672	NA	69248171
S006304	S006304_697561	X	59.908	NA	NA
S013985	S013985_11114	X	60.241	NA	82920002
	xd020	X	63.263	PcggcB53	NA
S007907	S007907_144642	X	64.648	NA	94604867
	xs011	X	67.511	PaaacA60	NA
S001930	S001930_1745657	X	68.641	NA	88122926
S001930	S001930_2410442	X	69.247	NA	88122926
S004832	S004832_609791	X	70.344	NA	91521965
S001247	S001247_68215	X	71.108	NA	92776928
	xs012	X	75.227	PaagcA53	NA
S000238	S000238_1169086	X	90.242	NA	113789231
S003071	S003071_613045	X	95.05	NA	116953618
S002737	S002737_694631	X	117.43	NA	NA
S000176	S000176_35913	X	126.585	NA	132559092
S001187	S001187_211572	X	130.879	NA	127829472
S003230	S003230_1425064	X	131.437	NA	129558233
S002008	S002008_1089204	X	131.468	NA	126707516

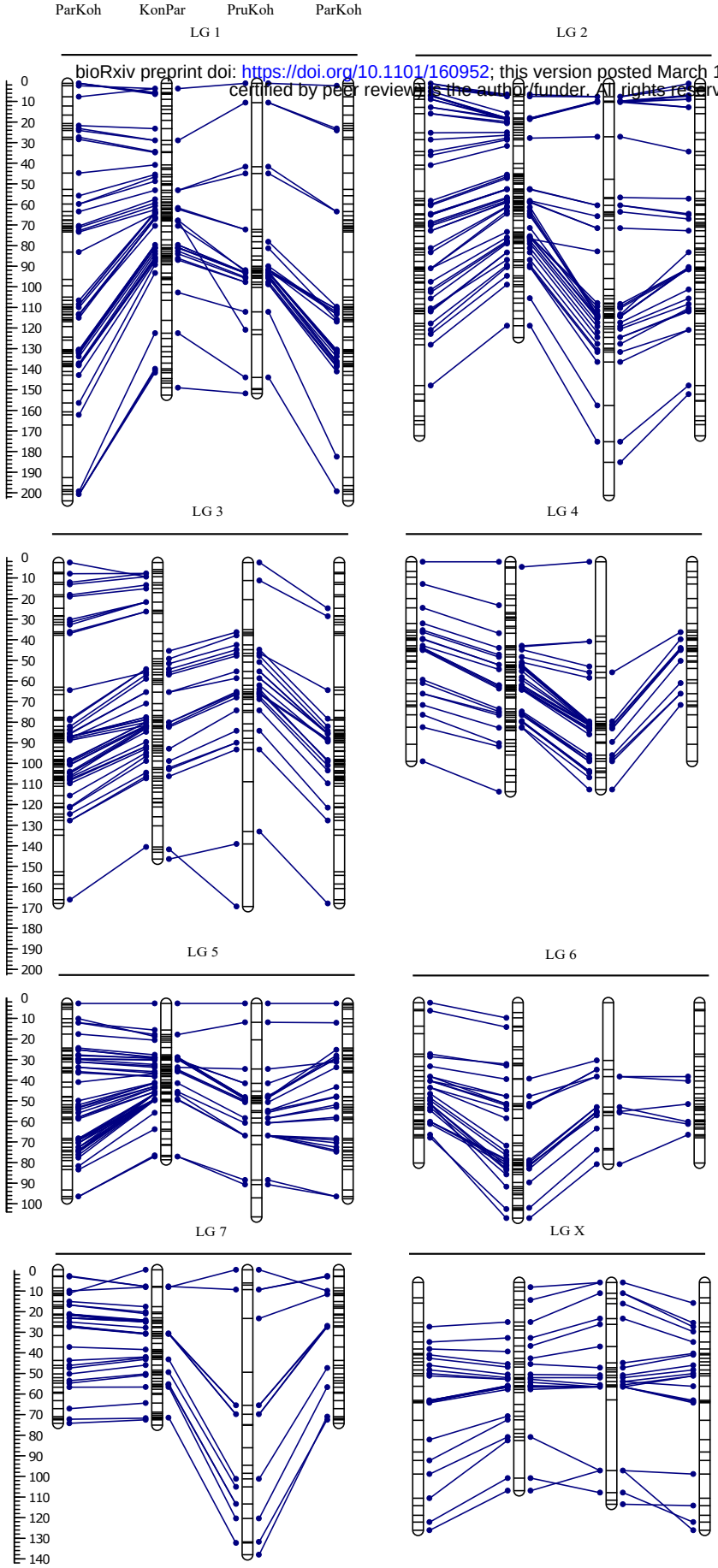

Figure S1.Comprehensive linkage maps. Bars represent linkage groups (LG) for ParKoh, KonPar, and PruKoh. Lines within the bars indicate marker positions. The scale on the left gives marker position in cM. Blue lines connect markers on the same scaffold between the different maps (homologous markers). The map for ParKoh is shown twice to facilitate comparisons across all three maps.

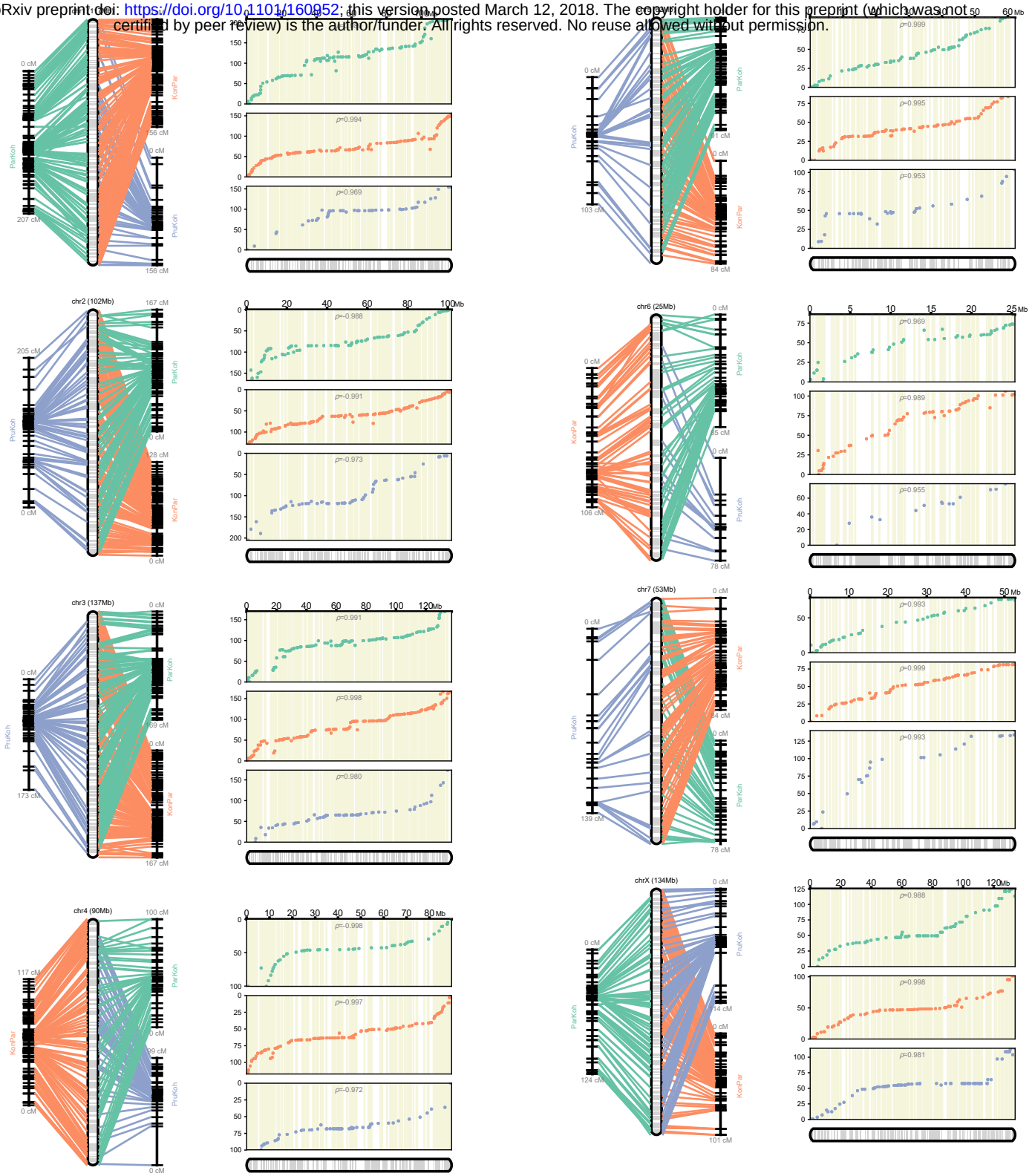

Figure S2. ALLMAPS output. For each of the linkage groups (chr) the relative order with respect to the shared map (i.e. the pseudomolecule assembly) is shown as well as Spearman's rho (ρ) for the strength of correlation between marker orders.

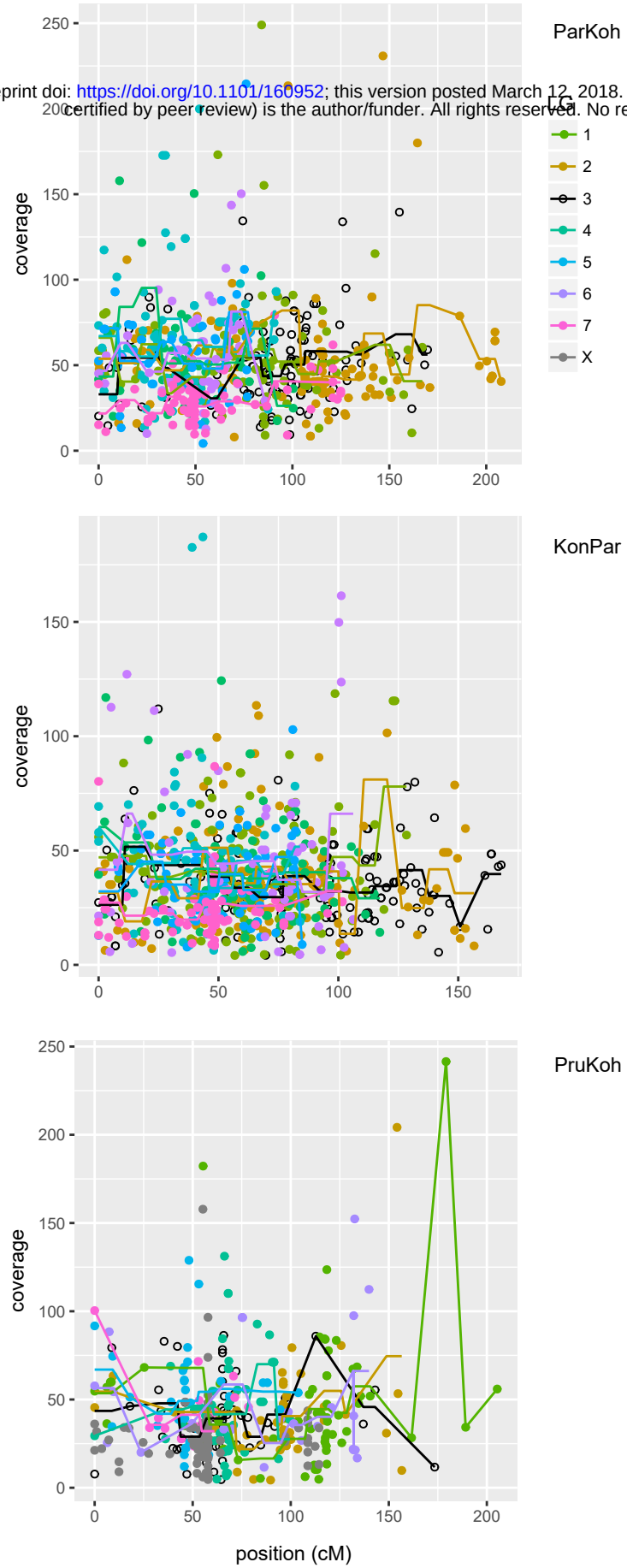

Figure S3. Coverage per cross per linkage group. For each of the three linkage maps (ParKoh, KonPar, PruKoh) the variation in coverage across the 8 linkage groups is shown. Coverage is calculated as the average (across individuals) read count per marker (points). Solid lines show 10-cM non-sliding window averages.